

1 Cyanobacterial Bloom Phenology in Saginaw Bay from MODIS and a comparative look with
2 western Lake Erie

3 Timothy T. Wynne¹, Richard P. Stumpf¹, R. Wayne Litaker², Raleigh R. Hood³

4 ¹ National Oceanic and Atmospheric Administration, National Ocean Service, National Centers
5 for Coastal Ocean Science, 1305 East-West Highway, Silver Spring, MD 20910, USA

6 ² CSS, Inc. Under contract with National Oceanic and Atmospheric Administration, National
7 Ocean Service, National Centers for Coastal Ocean Science, 1305 East-West Highway, Silver
8 Spring, MD 20910, USA

9 ³ Horn Point Laboratory, University of Maryland Center for Environmental Science, Cambridge,
10 MD USA.

11

12 Keywords: Dissolved Reactive Phosphorus, DRP; Western Lake Erie basin, WLEB, Saginaw
13 Bay, Cyanobacteria, Remote Sensing

14

15 **ABSTRACT**

16 Saginaw Bay and western Lake Erie basin (WLEB) are eutrophic catchments in the Laurentian
17 Great Lakes that experience annual, summer-time cyanobacterial blooms. Both basins share
18 many features including similar size, shallow depths, and equivalent-sized watersheds. They are
19 geographically close and both basins derive a preponderance of their nutrient supply from a
20 single river. Despite these similarities, the bloom phenology in each basin is quite different. The
21 blooms in Saginaw Bay occur at the same time and place and at the same moderate severity level
22 each year. The WLEB, in contrast, exhibits far greater interannual variability in the timing,
23 location, and severity of the bloom than Saginaw Bay, consistent with greater and more variable
24 phosphorus inputs. Saginaw Bay has bloom biomass that corresponds to relatively mild blooms
25 in WLEB, and also has equivalent phosphorus loads. This result suggests that if inputs of P into
26 the WLEB were reduced to similarly sized loads as Saginaw Bay the most severe blooms would
27 be abated. Above 500 metric tons P input, which occur in WLEB, blooms increase non-linearly

28 indicating any reduction in P-input at the highest inputs levels currently occurring in the WLEB,
29 would yield disproportionately large reductions in cyanobacterial bloom intensity. As the
30 maximum phosphorus loads in Saginaw Bay lie just below this inflection point, shifts in the
31 Saginaw Bay watershed toward greater agriculture uses and less wetlands may substantially
32 increase the risk of more intense cyanobacterial blooms than presently occur.

33 1. Introduction

34 Harmful Algal Blooms (HABs) are increasing worldwide (Smayda, 1990; Hallegraeff, 1993;
35 Paerl and Paul, 2012; Ho et al., 2019). In freshwater systems these blooms are dominated by
36 cyanobacteria, which adversely affect public health, water quality, and the normal food webs
37 found in healthy aquatic ecosystems (Brooks et al., 2016). In the Great Lakes, cyanobacteria
38 frequently produce potent hepatotoxins, such as microcystins (Watson et al., 2008; Brooks et al.,
39 2016). Additionally, they can make organic compounds, such as geosmin, that cause taste and
40 odor issues in municipal water supplies, a potential problem for residents that rely on Lake Erie
41 (USA) for drinking water. Since 2002, two drinking water advisories were issued due to
42 cyanotoxins, the most notable of these occurred in 2014, when the metropolitan area of Toledo,
43 Ohio went several days under a “Do not drink” order (Steffen et al., 2017). Cyanotoxins can also
44 cause mortalities in domestic animals as well as wildlife, primarily through ingestion of
45 cyanobacterial scums (Hilborn and Beasley, 2015). The cyanobacterial blooms in the western
46 basin of Lake Erie (WLEB) have been the focus of many studies using remotely sensed imagery
47 (Bosse et al., 2019; Gorham et al., 2017; Sayers et al., 2016; Stumpf et al., 2012; Stumpf et al.
48 2016; Wang et al., 2018; Wynne et al. 2008, 2010; Zhang et al., 2017). In contrast, relatively few
49 remote sensing studies have focused on Saginaw Bay, Michigan, USA (Budd et al., 2001; Sayers
50 et al., 2016).

51 Given this lack of information on bloom phenology in Saginaw Bay and the lower intensity
52 blooms relative to the WLEB, whose watersheds share many morphological similarities, the
53 current study was undertaken to address two primary objectives. The first was to describe the
54 bloom phenology of Saginaw Bay using satellite data. The second was to compare the remotely
55 sensed bloom phenology in Saginaw Bay with that of the more intensively studied WLEB to

56 determine if the same or different environmental and anthropogenic factors govern the
57 magnitude and timing of cyanobacterial bloom phenology in both systems. To accomplish these
58 objectives, 20-year time series of satellite derived cyanobacterial bloom biomass estimates for
59 both systems were calculated and used to produce bloom phenologies. The roles of phosphorus
60 (P) load, land use practices, water residence times, and other environmental factors in regulating
61 the observed cyanobacterial bloom phenologies were then evaluated. The input of phosphorus
62 into WLEB has been identified as critical to bloom size (Stumpf et al., 2012; Kane et al., 2014;
63 Obenour et al., 2014; Manning et al., 2019), while nitrogen (N) limitation has been identified as
64 a key factor in bloom toxicity (Horst et al., 2014; Gobler et al., 2016; Chaffin et al., 2018) and in
65 constraining the growth of late summer cyanobacterial blooms in Lake Erie (Chaffin et al., 2013,
66 2018). Saginaw Bay has not been as extensively studied as western Lake Erie. The Saginaw
67 River has phosphorus load measurements, but lacks measurements on nitrogen loading and as
68 such, the role of phosphorus on cyanobacterial biomass is the topic investigated here.

69 2. Materials and methods

70 A twenty-year time series of satellite derived cyanobacterial bloom estimates from the WLEB
71 and Saginaw Bay was calculated and used to characterize bloom phenology in each system. The
72 role of nutrient inputs, land use practices, water residence times, as well as other environmental
73 factors in governing the observed variability, timing and intensity of the cyanobacterial blooms
74 were examined. This comparison allowed assessment of whether the factors controlling bloom
75 dynamics appeared similar or different between the two systems. The spatio-temporal dynamics
76 of cyanobacterial blooms in Saginaw Bay were also examined in greater detail as these blooms
77 have been previously less well characterized compared to the WLEB.

78 2.1. *Western Lake Erie basin characteristics*

79 The WLEB, west of Pelee Point to Avon Point (Fig. 1, lower panel), is located approximately
80 215 kilometers south of Saginaw Bay (Fig. 1, middle panel). It occupies the westernmost portion
81 of the 25,740 km² surface area of Lake Erie and encompasses the area where cyanobacterial
82 blooms in the region develop. The WLEB has a surface area of 3,375 km². It is relatively warm,

83 shallow (mean depth of 7 m), and productive relative to the other Great Lakes. Approximately 12
84 million people, 1/3 of the population of the Great Lakes basin, reside within the Lake Erie
85 watershed. In addition to supporting the largest fisheries stocks, it is the most anthropogenically-
86 impacted portion of the Great Lakes (Steffen et al., 2014). The Maumee River watershed is the
87 largest watershed in the Lake Erie region covering 21,538 km² with a population of 278,000
88 residents.

89 In the 1970s, the chlorophyll levels in the WLEB were often extremely high, exceeding the 50
90 µg L⁻¹ range (Rockwell et al., 2005). The Maumee River is the main supply of nutrient-enriched
91 waters into the WLEB (Stumpf et al., 2012). The Detroit River, though having a much larger
92 discharge (~35 times), has much lower phosphorus concentrations than the Maumee River. In
93 addition to these low nutrient levels, the high dilution rates caused by the larger outflow
94 precludes development of significant cyanobacterial blooms within the Detroit River plume itself
95 (Wynne and Stumpf, 2015). As a result, the outflow of the Detroit River does not contribute
96 significantly to cyanobacterial blooms in the WLEB other than by transporting a portion of the
97 cyanobacterial population in Lake St. Clair to the WLEB via the Amherstburg Channel (Davis et
98 al., 2014). The predominant land use in the watershed (78%) is agricultural, primarily row crops.
99 Nearly the entirety of the WLEB watershed was once home to the approximately 4000 km²,
100 Great Black Swamp, which was drained for agriculture in the mid-19th century leaving the
101 WLEB nearly devoid of wetlands (Mitsch, 2017).

102 The Maumee River plays a primary role in regulating cyanobacterial bloom intensity in
103 WLEB through delivery of nutrients (Fig. 1; Stumpf et al., 2012; Kane et al., 2014; Obenour et
104 al., 2014;). Some lacustrine systems are limited by nitrogen (N) or phosphorus (P) or a
105 combination of both (Xu et al., 2009; Paerl and Otten, 2013; Paerl et al. 2016). In the case of
106 western Lake Erie, the literature indicates that the development and overall magnitude of
107 cyanobacterial blooms is primarily dependent on P-loading (Stumpf et al., 2012, 2016; Kane et
108 al., 2014, Obenour et al. 2014; Bertani et al., 2016; Manning et al., 2019). While, neither Stumpf
109 et al. (2012) nor Kane et al. (2014) found a relationship between N loads and cyanobacterial
110 bloom size in the WLEB, this does not eliminate the importance of nitrogen. Newel et al. (2019

111 implicated an increase in the ratio of annual loads of reduced N (Total Kjeldahl nitrogen; TKN)
112 to NO₃⁻ in the Maumee River to annual cyanobacterial bloom biomass, although they did not
113 examine the nitrogen loads for either form, and this time period also corresponded to an increase
114 in DRP load. However, other studies have examined the bloom response to nutrient enrichment
115 and found that N limitation occurs in the developed bloom in WLEB, (Chaffin et al., 2013;
116 Gobler et al., 2016; Chaffin et al., 2018). N-limitation also regulates bloom toxicity in WLEB,
117 constrains the growth of late summer cyanobacterial blooms, and likely influences bloom
118 duration and termination (Chaffin et al. 2013; Horst et al. 2014; Gobler et al. 2016; Chaffin et al.
119 2018; Boedecker et al. 2020). However, factors driving toxicity or duration are not part of this
120 study. Also, as a practical matter, there are no data sets for nitrogen loads to Saginaw Bay,
121 restricting us to examining phosphorus influence on bloom size or biomass. Given how close the
122 Saginaw Bay and WLEB are to one another, and their similarities in geomorphologies, we can
123 reasonably hypothesize that P-inputs play a similar role governing cyanobacterial bloom biomass
124 in Saginaw Bay as in WLEB.

125 2.2. Saginaw Bay characteristics

126 Saginaw Bay (Fig. 1, upper panel) is a large catchment in the southwestern portion of Lake
127 Huron in the Laurentian Great Lakes encompassing approximately 2,650 km². The Saginaw Bay
128 watershed is primarily drained by the Saginaw River. This watershed is the largest in the U.S.
129 state of Michigan and includes one of America's most extensive contiguous freshwater wetland
130 systems. Fifteen percent of the land in Michigan lies within the Saginaw Bay watershed, and is
131 home to approximately 1.5 million people. Most of these residents get their water from the
132 northwest side of Saginaw Bay about 50 km southwest of Au Sable Point (Saginaw 2020). The
133 land use within the watershed consists of 45% agriculture, 22% forest, 16% open water/wetland,
134 10% residential, 6% grassland, and 1% high density residential. Nearly the entire shoreline of the
135 bay is lined with dense stands of three square bulrush, (*Schoenoplectus pungens*). The
136 bathymetry of the bay is complicated (Fig. 1, upper panel), and makes for a complex circulation
137 pattern. The water enters Saginaw Bay from Lake Huron on the western side of the basin and
138 mixes with output from the Saginaw River before flowing along the eastern side of the bay and

139 returning to Lake Huron. This predominant flow is reinforced by a small island located in the
140 south central portion of the Bay that helps channel flow into and out of the Bay. The bottom
141 substrate in Saginaw Bay consists primarily of limestone and dolomite bedrock and large cobble.
142 The deeper outer portion of the bay, which mixes more completely with Lake Huron water, is
143 more oligotrophic, clearer, and colder relative to the inner bay.

144 Beginning in the early 1990s, Saginaw Bay was invaded by both zebra mussels
145 (*Dreissena polymorpha*) and quagga mussels (*Dreissena bugensis*) (Pillsbury et al., 2002;
146 Vanderploeg et al., 2001). Both species became well established and were a fundamental
147 component of the food web during this study period (Heath et al., 1995; Pillsbury et al., 2002).
148 Their presence is important because these species likely promote cyanobacterial blooms by
149 differentially consuming diatoms and other competing organisms (Vanderploeg et al., 2001). The
150 cyanobacterial blooms, though favored by differential grazing, are generally reported to be less
151 severe in Saginaw Bay (Fig. 1 upper panel, Sayers et al., 2016). The role of nutrients in
152 controlling cyanobacterial biomass in this system cannot be addressed with the same accuracy as
153 in the WLEB because only TP data are available for comparison (Cha et al., 2010; Stow et al.,
154 2014).

155 2.3. Satellite data

156 Imagery from the Moderate-resolution imaging spectroradiometer (MODIS) used to assess
157 cyanobacterial biomass was acquired from NASA. The MODIS sensor is onboard two separate
158 spacecraft: Aqua and Terra. Imagery from both satellites was used in this study. The MODIS
159 imagery was used to detect and quantify cyanobacteria blooms by applying the Cyanobacterial
160 Index (CI). This algorithm was originally derived for the Medium Resolution Imaging
161 Spectrometer (MERIS) (Wynne et al., 2008; Wynne et al., 2010; Wynne et al., 2013b), and is
162 described in Equation 1.

163 (eq. 1) $CI = (-SS(678)) * 1.33$

164 Where SS is the spectral shape (or curvature; Stumpf and Werdell, 2010) and is determined as

165 (eq. 2)
$$SS(678) = Rho_s(678) - Rho_s(667) - \{Rho_s(748) - Rho_s(667)\} * \frac{(678 - 667)}{(748 - 667)}$$

166 Where *Rho_s* is the top of atmosphere reflectance corrected for Rayleigh radiance (NASA, 2019)
167 and 1.33 in eq. 1 is a correction factor originating from Wynne et al. (2013b). *Rho_s* allows
168 potential data retrieval in conditions where the atmospheric correction might fail, such as areas
169 of high glint or aerosols (Gower and King, 2007). The standard cloud flagging procedure was
170 used to mask clouds (L2 flags; NASA, 2019, Wynne et al., 2018). Wynne et al. (2013b) showed
171 that the CI could be calculated from MODIS and that with proper corrections the MODIS CI is
172 equivalent to the MERIS CI. A similar correction should be possible with the relatively newly
173 launched Ocean Color Land Imager (OLCI). This will ensure data continuity to build a
174 climatological time series of cyanobacteria blooms in the Great Lakes when MODIS, which is
175 well beyond its mission life, fails. The CI algorithm has been used extensively in disparate water
176 bodies, including the WLEB (Wynne et al., 2010; Wynne and Stumpf, 2015; Wynne et al.,
177 2008), Saginaw Bay (Wynne et al., 2008); and various lakes in New England (Lunetta et al.,
178 2015), Ohio, and Florida (Mishra et al., 2019). More recently the algorithm has been applied to
179 lakes across the continental U.S. with successful results (Clark et al., 2017; Urquhart et al., 2017;
180 Schaeffer et al., 2015, 2018).

181 The red bands used in this algorithm penetrate pure water to about two meters due to red light
182 being strongly absorbed by water (Pope and Fry, 1997). The addition of material into the water
183 column will lessen the depth penetration of the algorithm to under a meter (and shallower still in
184 a cyanobacteria bloom). The spectral shape corrects for total albedo of shallow water, however,
185 it may detect benthic cyanobacteria (“algal mats”). Bottom effects were problematic in the very
186 shallow waters in areas of emergent land in eastern Saginaw Bay, near the Wildfowl Bay State
187 Wildlife Area. Whether due to actual interference or benthic cyanobacteria in this region the
188 wildlife area was included as part of the land mask to avoid potential interference due to benthic
189 cyanobacteria (Fig. 1). Sediment does not typically cause false positives in the CI. Hawley et al.
190 (2014) did an in-depth analysis on sediment resuspension in Saginaw Bay. A MODIS image with
191 particularly high resuspension was used as an example in their manuscript. The same image

192 showed no false positives with the algorithm employed in equation 1. The CI product has been
193 used for years in Lake Erie without evidence of impact due to resuspended sediments (Wynne et
194 al., 2012; Stumpf et al., 2016).

195 To analyze the data set, we partitioned the composites at 10-day intervals starting June 1 and
196 extending through October 31 (Table 1). This follows the convention used by Stumpf et al. (2012)
197 and Wynne and Stumpf (2015) and is based on the assumptions that the cyanobacteria are relatively
198 slow growing (estimated at $\sim 0.295 \text{ day}^{-1}$) and that during at least one day within the 10-day
199 window, winds will be low and atmospheric conditions will be cloud free. This growth rate estimate
200 is consistent with Wilson et al. (2006). They measured the maximal growth rates of numerous
201 *Microcystis aeruginosa* isolates and found an average of $0.27 \pm 0.02 \text{ day}^{-1}$ (range 0.14 to 0.46 day⁻¹)
202 ¹). Prevailing low winds allow cyanobacteria to accumulate at the surface, providing a better
203 estimate of overall cyanobacteria concentrations within the water column. Wynne et al. (2010)
204 showed that wind speeds where stress exceeds 0.1 Pascal (generated by winds $> 7.7 \text{ m s}^{-1}$) were
205 enough to mix the bloom through the water column so that the majority of the bloom material was
206 out of the detection limit of satellite (roughly a depth of 0.5 meters in bloom conditions).
207 Approximately 24 hours after the stress was removed cyanobacterial cells were able to redistribute
208 to the surface of the water, where accurate bloom biomass estimations from satellite could be made.
209 Because cyanobacteria prefer warm water temperatures, and Saginaw Bay often freezes in the
210 winter, the CI values were calculated only from satellite images obtained during the warmer
211 months.

212 For each 10-day period the maximum CI value at each pixel observed in any of the satellite images
213 for that time were retained to form a final “*composite*” image of maximum CI values at each pixel.
214 All subsequent references to CI will indicate a composite image containing these pixel-specific
215 maximum CI values for each 10-day period (Stumpf et al., 2012). CI values are useful for showing
216 the spatial distribution of maximum CI values for a given 10-day composite. Each month contained
217 three ten-day composites, so the third 10-day composite of a 31-day month was extended to
218 encompass 11-days. For simplicity, these 11-day composites are also referred to as “10-day”

219 composites (see Table 2 for details). In any CI data comparisons between Saginaw Bay and WLEB
220 the same 10-day periods were used.

221 *2.4. Interannual variability in bloom biomass*

222 To address interannual variability of cyanobacteria biomass in Saginaw Bay the following steps
223 were taken. Initially, for each available 10-day composite, the maximal CI values from every
224 pixel were summed to provide an overall or “integrated” biomass estimate (Stumpf et al. 2012).
225 This procedure produced 15 integrated CI estimates for each year between June 1 - October 31
226 (Table 1) from 2000 to 2019 in both Saginaw Bay and the WLEB. The largest of the 15
227 integrated CI biomass values each year was selected to represent the maximal annual biomass
228 value (Stumpf et al., 2016). Cyanobacterial blooms in Saginaw Bay were retained within the Bay
229 and only the pixels covering the 2,650 km² surface area were included in each scene. In contrast,
230 blooms originating in the WLEB are sometimes transported into the central basin to the area near
231 Avon Point (Fig. 1, lower panel). To capture this transport, satellite surveillance of blooms was
232 extended beyond WLEB proper to include the areas west of a line between Pelee Point and Avon
233 Point. This region has a surface area of 4,983 km². Hereafter, bloom in "the WLEB" will refer to
234 cyanobacterial blooms that originated in the shallow basin proper plus biomass exported out of
235 the basin captured in the satellite imagery. The goal was to encompass all the biomass
236 originating within WLEB proper, but to exclude any blooms developing independently in the
237 central basin of Lake Erie.

238 *2.5. Bloom maxima in Saginaw Bay and western Lake Erie Basin*

239 Given the similarities between Saginaw Bay and WLEB, a logical question to address is whether
240 blooms in each develop and peak at the same or different times during the summer. To address
241 this question, statistics (mean, standard deviation, mode, and median) describing the time period
242 where the maximum CI value occurred were then determined for the integrated CI values for
243 each 10-day period (e.g., June 1 to June 10) over all 20 years (Table 1).

244 *2.6. Relationship of total phosphorus (TP) inputs and subsequent cyanobacterial bloom biomass* 245 *in Saginaw Bay and the western Lake Erie basin*

246 Total bioavailable phosphorus (TBP), which consists of DRP and the fraction of the particulate
247 phosphorus that is bioavailable, is the primarily P-source used by cyanobacteria in the WLEB
248 (Baker et al., 2014) and what regulates bloom biomass (Stumpf et al., 2016; Manning et al.,
249 2019). Because TBP and TP are highly autocorrelated (Supplementary Fig. 1; $r^2=0.91$), both P
250 measurements have been successfully used to predict P-loading and cyanobacterial bloom
251 biomass in the WLEB (Stumpf et al., 2012; Obenour et al. 2014; Kane et al., 2014; Bertani et al.,
252 2016). For Saginaw Bay TP, but no DRP, data are available. For this reason, TP was used as the
253 comparable measurement of P-loading in both Saginaw Bay and the WLEB allowing the
254 subsequent examination of the relationship between P-inputs and cyanobacterial biomass
255 production. Total phosphorus is also generally used to set limits for eutrophication because it is
256 the form most commonly and readily measured so the results can be directly related to existing
257 water quality standards (GLWQANAS, 2019).

258 *2.6.1. River discharges*

259 The Saginaw River, and the Maumee River are the primary sources of nutrients driving
260 cyanobacterial growth in both systems (Newell et al., 2019; Baker et al., 2014; Stumpf et al.,
261 2012; Withers and Jarvie, 2008). Within the Saginaw Bay watershed, the Saginaw River is by far
262 the largest source of water flowing into the bay contributing ~70% of the freshwater input (Stow
263 et al., 2014) and ~90% of the nutrient load (Bierman et al., 1984). Likewise, the Maumee River
264 is a key source of the nutrients entering WLEB, and along with the much smaller Cuyahoga and
265 Sandusky Rivers contribute 50% of the P load into Lake Erie (Baker et al., 2014). Consequently,
266 any differences in the magnitude in timing of water discharges from the Saginaw and Maumee
267 Rivers can potentially affect timing and magnitude of cyanobacterial blooms. To document any
268 differences in discharge patterns between the two rivers, Saginaw River flow measurements were
269 obtained from the United States Geological Survey's (USGS) gage station 04157005 at Holland
270 Avenue at Saginaw, MI, and those for the Maumee River from the USGS gage station 04193500
271 at Waterville, Ohio. The resulting data were utilized as described in the sections 2.6.2 and 2.6.3.

272 *2.6.2. Estimating what period of river flow best correlated with the 10-day maximum CI value in*
273 *Saginaw Bay*

274 Research on cyanobacterial blooms in the WLEB demonstrated flow and TP inputs from March -
275 June best predicted maximum cyanobacterial biomass later in the summer (Stumpf, 2012;
276 Obenour et al. 2014). Stumpf et al. (2016) found that July loads also mattered when the mean
277 water temperature in June was greater than 20 °C. It is not known which period of river flow best
278 correlates with cyanobacterial biomass in Saginaw Bay. To address this question, we examined
279 four different integrated periods of river discharge ($\text{m}^3 \times 10^9$). These were: (1) The water year
280 (October - September), (2) March - June, (3) March - July, and (4) January-April. The October -
281 September time period reflects the TP input starting from the termination of cyanobacterial
282 blooms by early October of the previous year through the bloom maximum the next summer as
283 well as the termination of the bloom in September. Outflow for these various time periods each
284 year were compared to the corresponding maximal integrated 10-day CI (maximal biomass)
285 value for that year (section 2.4). This made it possible to perform regression analyses to
286 determine if the volumetric out flow from the Saginaw River for any of the different time periods
287 better correlated with maximal cyanobacterial biomass.

288 Additionally, a direct comparison of the average river discharge patterns in Saginaw Bay
289 and the WLEB was also undertaken to establish how similar or different the pattern of monthly
290 discharge was in the two water bodies. This was accomplished by determining the mean
291 monthly water discharge volume for both rivers from 2000-2019. The data were analyzed from
292 October to September which corresponds with the annual bloom progression observed in
293 Saginaw Bay and Lake Erie.

294 *2.6.3. TP loading in Saginaw Bay and Western Lake Erie Basin*

295 TP loads for the Maumee River are available from Heidelberg University's National Center for
296 Water Quality Research (NCWQR) (Heidelberg University, 2019) from 1975 to the present. For
297 Saginaw Bay, the only TP-loading data available are from the study by Cha et al. (2010), which
298 modeled the TP from 2000-2008. That study utilized known phosphorus concentrations, river

299 flow rates, and loading estimates directly measured by Michigan Department of Environmental
300 Quality or obtained from other sources from 1974 - 1991 and 2001 - 2005 (MDEQWB, 2010).
301 Those data allowed development of a Bayesian model predicting the TP loads from flow rates.
302 This model, along with flow rates from the USGS allowed continuous estimation of loading from
303 1968-2008, despite the lack of measured nutrient concentration data in some years. The last 9
304 years of the Cha et al. (2010) data set overlap with the first 9 years of this study. As a result, it
305 was only possible to obtain estimates of TP concentrations for the period between 2000-2008.
306 How P-loading drives cyanobacterial blooms in both Saginaw Bay and the WLEB was therefore
307 limited to this nine year time period.

308 The cumulative TP loading for each year for the Saginaw from 2000-2008 was calculated from
309 the Cha et al. (2010) data using the following equation:

310

311 (eq. 3)
$$TP = \sum_{i=March}^{n=June\ 30} (TP_T \times q_i / Q_T)$$

312 Where TP is the total phosphorus input from March to June, TP_T is the TP load for the year in
313 metric tons, q_i is the discharge for the month i , and Q_T is the total discharge for the year for the
314 Saginaw River calculated from sources described in section 2.4.1, and i is month (Sigleo and
315 Frick, 2003).

316 *2.7 Changes in TP concentrations in the Saginaw River over time*

317 Baker et al. (2014) showed a decrease in TP loads from the Maumee River over time from the
318 1970s to 1990s as abatement measures were put into effect. The degree to which P-loading in
319 Saginaw Bay has declined over the same time, if any, has been less well studied. To determine if
320 a corresponding decline in TP inputs also occurred in Saginaw Bay, two studies done almost a
321 decade apart were analyzed. Specifically, the regression equation for the relationship between
322 annual volumetric discharge from the Saginaw River and annual TP loading for the periods 1974
323 - 1991 and 2001 - 2005, respectively, were analyzed. The data used in the analysis were collated
324 from different sources by the Michigan Department of Environmental Quality Water Board

325 (MDEQWB, 2010; Supplementary Fig. 2). The slope of each regression line corresponded to the
326 average flow weighted mean concentration (FWMC) for each period. Changes in the FWMC
327 were indicative of how loading has changed in response to abatement efforts. The relationship of
328 annual output from the Saginaw River versus TP loading from 1974 - 1991 shows an average
329 FWMC of 0.27 mg L⁻¹ (from the slope) versus 0.17 mg L⁻¹ for the 2001 - 2005 period
330 (MDEQWB, 2010) (Supplementary Fig. 2). This difference indicates a 37% drop in average
331 FWMC of TP in response to efforts to reduce loading as of 2005, which shows the efficacy of P-
332 reduction efforts in the Saginaw Basin. It also indicates the relationship between TP load and
333 discharge (FWMC) changed such that the same models may not be applicable to both current
334 and historical conditions.

335 2.8. Modeled maximum, cumulative 10-day CI predicted from total phosphorus (TP) loading

336 To assess the similarity or differences in response to P-inputs in Saginaw Bay and WLEB, we
337 used a modified version of the model previously developed for western Lake Erie by Stumpf et
338 al. (2016). That model predicts cyanobacterial biomass based on a given March to June TP input.
339 Using the model and annual March to June TP loading values for 2000-2008, it is possible to
340 calculate expected maximal cyanobacterial biomass for each year of the study. A comparison of
341 the modeled versus actual maximal biomass estimates can be used to evaluate if equivalent TP
342 loading in Saginaw Bay produces the same amount of cyanobacterial biomass as occurs in the
343 WLEB and if the modeled results agree well with the measured maximal cyanobacterial biomass
344 estimated from satellite imagery. The modeling procedure is given below.

345 The model developed by Stumpf et al. (2016) equating phosphorus load to total cyanobacterial
346 biomass in CI “units” (CI_{MERIS}) using the existing MERIS and adjusted MODIS data is:

347 (eq. 4)
$$CI_{MERIS\ model} = B \times 10^{a \times X}$$

348 Where $CI_{Meris\ model}$ = modeled CI value, $a = 7.48 \times 10^{-4}$, $B = 0.57$ and X = total phosphorus load in
349 metric tons for March-June estimated in section 2.6.3. As the MERIS sensor failed it was
350 replaced by the MODIS sensor. This transition required recalibration of the MERIS algorithm
351 from Stumpf et al. (2016) to fit the MODIS data used in this study because the MERIS

352 composited imagery had CI_{max} values slightly lower than the MODIS CI_{max} values for
353 overlapping scenes. This was particularly true of the 2011 bloom in which MODIS experienced
354 saturation of the sensor in scum areas (Wynne et al., 2013b). The algorithm that was used to
355 estimate the CI in the scum areas most likely overestimated the CI relative to MERIS, which
356 does not have a saturation issue (Wynne et al., 2018). Equation 4 needed to be recalibrated to
357 account for these differences. The CI MERIS from Stumpf et al. (2016) was plotted against with
358 the CI_{MODIS} in this study (Supplementary Fig. 3) and the resultant equation was

359 (eq. 5)
$$CI_{MODIS} = 0.81 \times CI_{MERIS} - 1.3$$

360 Combining equations 4 and 5 yields the following equation for $CI_{MODIS\ model}$

361 (eq. 6)
$$CI_{MODIS\ model} = B_{MODIS} \times 10^{a \times X} + 1.6$$

362 where a remains = 7.48×10^{-4} , $B_{MODIS} = 0.70$, with X = total phosphorus load in metric tons. For
363 Saginaw Bay and WLEB, the March-June TP loading values previously determined in section
364 2.4.3 were inserted into eq. 6 to calculate maximal 10-day $CI_{modeled}$ values for both Saginaw Bay
365 and WLEB from 2000 - 2008.

366 2.9. Effects of other forcing functions on bloom dynamics in Saginaw Bay

367 Other environmental factors besides P-input can modulate cyanobacterial bloom intensity in the
368 two systems. The factors that were considered in this study included cloud cover, incoming
369 shortwave irradiance (proxy for incoming photosynthetically active radiation), water
370 temperature, and wind stress (intensity and direction). Differences in average light availability
371 are associated with latitude and cloud cover, both of which may affect the growth of
372 cyanobacteria that often prefer high light. Water temperature was chosen because cyanobacteria
373 growth is strongly influenced by temperature (Paerl and Huisman, 2008). Wind stress was
374 chosen because it can affect the vertical distribution of cells and vertical migration directly
375 affecting CI values that only come from the top meter or so of the water column (Reynolds et al.,
376 1987; Wynne et al., 2010).

377 To examine how well these environmental factors correlated with bloom biomass, the June-
378 October data for the factors listed above were downloaded as climatological monthly means
379 from NASA's Giovanni reanalysis dataset (Giovanni, 2020) for the years 2000 to 2019. These
380 included products from the AIRS 1-degree cloud fraction, the MERRA-2 model (incoming
381 shortwave flux, surface wind stress), and the water temperature from the MODIS nighttime 11-
382 micron 4 km data. The corresponding CI scenes were binned to create monthly composites
383 instead of the 10-day integrated CI composites used elsewhere in this study. Once the June-
384 October monthly values were calculated, single parameter correlations were then performed
385 using the monthly CI and environmental data.

386 *2.10. Bloom phenology in Saginaw Bay*

387 The following analyses were performed to provide a more detailed resolution regarding the
388 temporal and spatial distribution of Saginaw Bay cyanobacterial blooms, which have been less
389 well investigated than those in western Lake Erie. The analyses were begun by first segregating
390 all the scenes from 2000-2019 into 15 datasets each containing the scenes for the same 10-day
391 period each year (Table 1). Each of the 15 datasets was then analyzed separately. CI values from
392 each corresponding pixel from all 20 scenes (2000-2019) in each data set were identified,
393 averaged and plotted as a single composite image showing the average CI distribution across
394 Saginaw Bay for that 10-day period. The resulting 15 composite plots of average CI values
395 across Saginaw Bay for each 10-day period were then presented in chronological order to show
396 the seasonal bloom progression from the summertime initiation to the final demise in the fall.
397 This analysis included any bloom where the CI is above the detection limit, i.e. > 0 , which is
398 estimated to be $\sim 10,000 - 20,000$ cells mL^{-1} (Davis et al., 2018).

399 In addition, two frequency analyses previously used to investigate bloom severity in WLEB were
400 performed (Wynne and Stumpf, 2015). The 2000-2019 MODIS imagery were used to illustrate
401 the bloom phenology described above and were partitioned into the same 15 datasets containing
402 the scenes for specific 10-day composite images from the first 17 years of the study. However,
403 instead of using the data to calculate an average composite pixel CI value, the data for each year
404 was examined to determine how many years during the time series the CI value for each pixel

405 exceeded a defined threshold value. The number of years where the threshold exceeded the
406 prescribed threshold value was then divided by 17 and multiplied by 100 to provide a frequency
407 estimate ranging from 0 to 100 percent. In the first frequency analysis, the threshold value was
408 $CI = 0$ as defined above. The resulting 15 frequency plots for each 10-day period were presented
409 in chronological order to show how frequently a bloom with $CI > 0$ was present in each section
410 from spring (June 1) to fall (Oct 31). The second analysis was performed in exactly the same
411 manner, but used a threshold value $CI \geq 0.001$, equivalent to a concentration of $\sim 10^5$ cells mL^{-1}
412 (Stumpf et al., 2012). This is the concentration recommended by the World Health Organization
413 as the upper limit for recreational exposure to cyanobacteria (Chorus and Bartram, 1999) and
414 represents the frequency of severe blooms throughout Saginaw Bay on average over the bloom
415 season. By analyzing the frequency of severe blooms only, the noise in the data is reduced.

416 *2.11. Spatial distribution of blooms in Saginaw Bay relative to the prevailing circulation pattern*

417 Another understudied aspect of the cyanobacterial blooms in Saginaw Bay is their spatial
418 distribution. The predominant flow in Saginaw Bay consists of water entering from Lake Huron
419 along the western side of the Bay and exiting along the eastern shore. This flow is reinforced by
420 an island located in the approximate center of the Bay that helps channel flow into and out of the
421 Bay. To determine how this flow pattern might influence spatial differences in the bloom
422 intensity, Saginaw Bay was divided into five different subregions. These included: (1) the area
423 closest to the river mouth at the southern end of the Bay, (2) the inner and (3) outer regions on
424 the eastern side of the Bay and (4) the inner and (5) outer regions along the western side.

425 Previous studies have similarly partitioned the Bay into these same subregions as a means of
426 documenting spatial differences in various biological measurements associated with differences
427 in depth and circulation patterns (Bierman et al., 1984; Fishman et al., 2010). The integrated CI
428 for each subregion for each 10-day composite period (Table 1) were then determined from the
429 MODIS data and shown as a separate time series from 2000-2019.

430 To further quantify interannual variability in bloom intensity among the different subregions of
431 Saginaw Bay, an integrated CI value for each year between 2000-2019 for each subregion was

432 determined. The annual subregional, integrated CI values were then normalized to the surface
433 area of each corresponding subregion (integrated CI km⁻²).

434 **3. Results**

435 *3.1. Satellite-derived interannual variability*

436 Every year during the 2000-2019 study period Saginaw Bay experienced a cyanobacterial bloom
437 (Figs. 1 and 2A). The magnitude of these blooms, as indicated by the largest integrated CI value
438 (biomass) during a 10-day period, showed relatively little interannual variation. The largest 10-
439 day integrated biomass estimate for the entire Bay occurred from 1-10 September, 2017. The
440 smallest bloom maximum occurred between 1-10 August, 2016. These maximum and minimum
441 bloom biomasses indicated blooms varied by no more than 4.25-fold interannually. If the 2017
442 maximum biomass value is excluded, the interannual variation drops to a 1.6-fold difference. In
443 contrast, blooms in the WLEB exhibited a much higher degree of interannual variability during
444 the same period. Maximal 10-day biomass estimates in this system ranged from an integrated CI
445 of 1.5 in 2005 to CI of 40 in 2011, corresponding with a 27-fold interannual difference in bloom
446 concentrations. If 2011 (which was the largest annual bloom, according to the methods described
447 here) is excluded, the interannual variation was still 15-fold. Figure 2B shows the maximum
448 integrated CI values for the same 10-day composites in Saginaw Bay superimposed over the
449 WLEB integrated CI. Blooms in WLEB during “minor bloom years” (2000-2002; 2005-2007)
450 were of similar magnitude to those in Saginaw Bay. Starting in 2008, the magnitude of the
451 cyanobacterial blooms in the two systems diverged. While the magnitude of blooms remained
452 relatively stable in Saginaw Bay, much larger blooms began to develop in WLEB during the
453 years 2008-2009, 2011, 2013-2015 and 2017. This divergence corresponded to a shift from drier,
454 more low flow years on average (2000-2008) to wetter years with generally higher flow rates
455 (2009-20017, 2019; Figs. 2B, 3).

456 *3.2. Timing of bloom maxima in Saginaw Bay and western Lake Erie Basin*

457 The mean, median, and mode of integrated CI values for each of the 10-day periods
458 (Table 1) over the course of the times series were determined, as was the 10-day period having

459 the highest mean, median, and mode values over the time series (Table 2). The mean, median,
460 and mode results all showed that the blooms peaked in Saginaw Bay about 20 days before those
461 in WLEB. Corresponding mean monthly water temperature estimates for 2002-2019 from the
462 USGS discharge stations from the Maumee River and the Saginaw River indicate the warmest
463 10-day period in both rivers occurred from 21 July - 31 July. The maximal temperatures,
464 however, were slightly different between the two systems. Mean monthly water temperatures for
465 WLEB were 24.0 °C in July, 24.2 °C in August and 21.6 °C in September, compared to 21.7 °C
466 in July, 22.0 °C in August and 19.4 °C in September for Saginaw Bay. Supplementary Fig. 4
467 shows the tight correlation and a slope near unity of the mean monthly surface water
468 temperatures between WLEB and Saginaw Bay.

469 *3.3. Flow period that best corresponds with maximum 10-day integrated CI value*

470 The Saginaw River was weakly correlated with the Saginaw Bay annual cumulative CI among
471 the time periods of March - June, March-July, January - April, and the water year (Fig. 3; R^2
472 ~ 0.2). Consequently, flow rate and associated nutrient loading estimates for Saginaw Bay were
473 integrated from March - June. This timeframe is as good as any other for predicting
474 cyanobacterial biomass in Saginaw Bay and is the period where river flow and TP loading best
475 correlate with maximal cyanobacterial biomass in the WLEB from 2000-2009 (Stumpf et al.,
476 2012). Integrating loading and flow over the same March - June period also simplified
477 comparisons of the mechanisms driving cyanobacterial blooms in both systems.

478 The average annual discharge pattern for the Saginaw and Maumee Rivers were similar with
479 peak flow occurring in April in the Saginaw River and March in the Maumee River (Fig. 3).
480 Though the pattern was similar, average discharge volumes from the Maumee River in March
481 were substantially higher than from the Saginaw River. April and May discharges from both
482 rivers were equivalent while those in June were again substantially higher from the Maumee
483 River. As a result, on average the overall discharge volume from the Maumee River is higher
484 than that from the Saginaw River. Another major difference between the two rivers was the
485 larger interannual variation relative to mean flow in the Maumee River, particularly between
486 March and July (Fig. 4).

487 *3.4. Relationship between the estimated March-June TP loading versus subsequent maximal 10-*
488 *day composite CI values*

489 The relationship between TP loading from the Saginaw and Maumee Rivers versus resultant
490 maximal cyanobacterial biomass was calculated as detailed in section 2.5. The volumetric
491 discharge of the Saginaw and Maumee Rivers during the drier period from 2000-2008, for which
492 TP data for the Saginaw River are available, were similar. In contrast, the amount of
493 cyanobacterial biomass produced for the same amount of river discharge was not equivalent. As
494 March - June outflow increased in the Saginaw Bay, the cyanobacterial biomass rose in a linear
495 fashion. In contrast, as discharge exceeded about $2 \times 10^9 \text{ m}^3$, cyanobacterial biomass in WLEB
496 increased in a non-linear fashion with the linear increases in flow producing progressively and
497 disproportionately more intense blooms compared to Saginaw Bay (Fig. 5A).

498 The plot of March - June TP inputs versus maximal cyanobacterial biomass showed a different
499 pattern than observed for river discharges (Fig. 5B). TP inputs between 110 to 400 metric tons
500 caused similar, linear increases in maximal bloom intensity in both Saginaw Bay and WLEB. TP
501 input into Saginaw Bay for 8 of the 9 years examined fell below this cut off point. The remaining
502 year received TP inputs of only 450 metric tons. TP inputs into WLEB exceeded 400 metric tons
503 for 7 of the 9 years with maximal loading exceeding 1,050 metric tons. As loading levels
504 exceeded 450 metric tons of TP in the WLEB, linear increases in TP produced a non-linear
505 response of progressively more intense cyanobacterial blooms (Fig. 5B).

506 *3.5. Modeled CI as a function of TP*

507 The modeled cyanobacterial biomass based in March - June TP input fell along a 1:1 line for
508 both Saginaw Bay and WLEB (Fig. 6). This is consistent with the model having been developed
509 for WLEB, which takes into account the non-linear response with increased TP loading. Because
510 the Saginaw Bay loading values were low, they fell in the more linear portion of the model
511 consistent with the observations in Fig. 5B. The tight clustering of points in Saginaw Bay are
512 also consistent with the low interannual variation in bloom intensity compared to the much larger
513 dynamic range for the WLEB. When interpreting these data, it should be noted that the Maumee

514 River Basin entered a wet phase in 2008 (Fig. 2B) and that is the only wet year included in this
515 analysis. As a result of this wet phase, TP loading for 2009 - 2019 for the Maumee River was
516 much greater, however, the corresponding TP measurements were not available for the Saginaw
517 River (Stumpf et al., 2016).

518 *3.6. Additional forcing functions effects on bloom dynamics in Saginaw Bay*

519 The single regression analyses of cloud cover, incoming shortwave irradiance, mean water
520 temperature and wind stress (intensity and direction) versus CI were conducted. Results revealed
521 that no single input parameter had a correlation above 0.05 to the integrated CI value.

522 *3.7. Bloom phenology and intensity in Saginaw Bay*

523 The average CI patterns from each 10-day composite for the entire 20-year time series is shown in
524 Fig. 7 for Saginaw Bay. The blooms peak in August, and subside relatively quickly in early
525 September. This differs from the WLEB, where a similar analysis showed peak concentrations in
526 mid-September (Wynne and Stumpf, 2015). Blooms are primarily distributed along the shoreline
527 every year forming a halo that does not fully extend into the center of the bay. Nguyen et al. (2014)
528 showed the prevailing current field in Saginaw Bay has strong divergent currents in the center
529 portion of the bay that move water away from the center of the bay towards the shore, which
530 prevents the cyanobacterial cells from accumulating there. These currents are particularly strong
531 in July and August, when the blooms are at their peak. The frequency of all blooms ($CI > 0$) per
532 10-day composite are shown in Fig. 8A, and the severe blooms ($CI > 0.001$) are shown in Fig. 8B.
533 These analyses also show the same pattern as observed in Fig. 7 with nearshore areas clearly
534 experiencing more blooms on average. In combination these results show blooms reliably initiating
535 in July, reaching peak in mid-August, fully dissipated by October and disproportionately impacting
536 areas adjacent to shore.

537 *3.8. Quantifying magnitude of cyanobacterial blooms in subsections of Saginaw Bay*

538 To examine differences in bloom intensity along various segments of the shoreline in Saginaw
539 Bay, the integrated CI values were calculated for 5 different subregions of Saginaw Bay for the

540 entire 20-year time series (Fig. 9B). The time series again revealed the same relatively invariant
541 pattern of annual blooms across the entire study period (Fig. 9A). The subsection where the
542 Saginaw River enters Saginaw Bay exhibited the highest composite CI values and the inner Bay
543 had generally higher CI values than the outer Bay. There was also an across Bay gradient in CI
544 values with Regions 2 (inner Bay) and 4 (outer Bay) along the western shore exhibiting lower CI
545 values than the corresponding subregions 3 (inner) and 5 (outer) along the eastern shore (Fig.
546 9C). This general pattern in cyanobacterial bloom intensity again corresponds with inflowing
547 oligotrophic waters from Lake Huron preferentially diluting the cyanobacteria bloom along the
548 western shore and outflowing currents differentially transporting bloom populations from near
549 the mouth of the Saginaw River along the eastern shore. A minor portion of the observed CI
550 differences may also be partially due to regions on the western side of the Bay having a lower
551 percentage of coastal adjacent pixels relative to the two regions on the eastern part of the bay.
552 Pixels immediately along the shoreline can sometimes have bottom reflectance or other
553 adjacency issues that cause overestimated CI values.

554 4. Discussion

555 4.1. *Factors governing severity and variability of cyanobacterial blooms in Saginaw Bay and the* 556 *western Lake Erie Basin (WLEB).*

557 The interannual differences in the variability and intensity of cyanobacterial blooms observed in
558 the WLEB relative to Saginaw Bay were extreme given both watersheds are similarly sized and
559 have a close geographic proximity. Saginaw Bay experienced relatively moderate, similarly
560 sized, cyanobacterial blooms each year between 2000-2019. In contrast, blooms in the WLEB
561 ranged from the intensities observed in Saginaw Bay to an order of magnitude higher (Figs. 1, 2).
562 Many of the larger WLEB blooms caused significant adverse impacts (Michalak et al., 2012;
563 Stumpf et al. 2016). The differences in bloom intensity were largely driven by two factors: the
564 greater flow weighted mean concentrations (FWMC) of TP in the Maumee River and the higher
565 and more variable volumetric discharge from the Maumee River (Figs. 3-5). The estimated
566 FWMC for TP in the Maumee is 0.36 mg L⁻¹ from 2000-2008 based on Stumpf et al. (2016) and
567 only 0.17 mg L⁻¹ for Saginaw Bay (Supplementary Fig. 2B). The impact of the differences in

568 FWMC of TP on cyanobacterial bloom formation was evident in comparing the influence of
569 discharge and TP on the maximal summertime biomasses in Saginaw Bay and the WLEB (Fig.
570 4). During this relatively dry 9-year period, the range in annual discharge volumes was
571 equivalent for these two similarly sized watersheds. Yet the same volumetric discharge from the
572 Maumee River produced more intense cyanobacterial blooms than equivalent discharges by the
573 Saginaw River (Fig. 5A). In contrast, when maximal biomasses in Saginaw Bay and the WLEB
574 were plotted versus the total March-June TP loading for both the Saginaw and Maumee Rivers,
575 comparable loading produced equivalent cyanobacterial biomass in both systems (Figs. 4B, 5A).
576 Blooms in Saginaw Bay clustered at the low end of the TP input range and were tightly grouped
577 reflecting the small interannual variation in TP inputs and resulting blooms. The largest variation
578 in cyanobacterial biomass occurred in the WLEB during the wetter period from 2009-2019, and
579 was again driven by much greater variations in May-June phosphorus loads from the P-enriched
580 Maumee River compared to the less enriched Saginaw River (Figs. 2B, 4; 5B, 6; Stumpf et al.
581 2016).

582 The higher nutrient load in the Maumee River is due to approximately 78% of the land use being
583 devoted to agriculture compared to 45% in the Saginaw Bay watershed (Ohio EPA, 2008). Most
584 of the agriculture in both watersheds is devoted to cultivation of row crops (corn and soybeans).
585 The soil types in both basins require drainage to make them agriculturally productive. As
586 fertilizers became commonly utilized, excess P was released into streams and rivers connected to
587 these drainage systems. Historically, efforts were undertaken in the 1970s and 1980s to reduce
588 the total load of TP into Great Lakes watersheds as a means of reducing the intensity of
589 cyanobacterial blooms. Significant progress was made toward meeting this goal during this
590 period (Baker et al., 2014). Then, in the 1990s a major shift in agricultural practices occurred in
591 the Maumee and Saginaw River watersheds with the widespread adoption of no-till farming with
592 fertilizer being directly applied to the soil surface (Smith et al., 2015a; Jarvie et al., 2017). A
593 major goal achieved using this approach was to stabilize or reduce export of particulate P to
594 streams and lakes (Jarvie et al. 2017). Adoption of the no-till farming practices required large-
595 scale installation of tile drainage systems in the Saginaw and Maumee watersheds as a way to
596 maintain more optimal soil moisture levels. A major unintended consequence documented the

597 Maumee River was a doubling in dissolved reactive phosphorus (DRP) load from the mid-1990s
598 to early 2000s while particulate phosphorus (PP) remained relatively constant (Baker et al.,
599 2014; King et al., 2015a; Smith et al., 2015a; Stow et al., 2015; Williams et al., 2016; Baker et al.
600 2017; Jarvie et al. 2017). The DRP export from tile drainage systems accounted for >90% of all
601 measured concentrations exceeding recommended levels for minimizing cyanobacterial blooms
602 (King et al., 2015b). This increased DRP input, which is immediately utilizable by
603 phytoplankton for growth, more than any other factor resulted in a re-eutrophication of the
604 WLEB and contributed greatly to increased cyanobacterial biomass in the WLEB (Young et al.,
605 1985; Kane et al., 2014; Smith et al., 2015b; Verhamme et al., 2016). It should be noted that not
606 all nutrient loading is from row crop agriculture, and that Concentrated Animal Feeding
607 Operations (CAFOs) are on the rise. We chose to focus on the larger and better documented
608 source of nutrients into the system, which is row crop agriculture.

609 In contrast, measured TP levels in the Saginaw River Basin where forests and wetlands account
610 for 22% and 16% of land cover, respectively, remain relatively low (Fig. 5B). Maintenance of
611 relatively low P concentrations over time in the Saginaw River is further supported by the 37%
612 drop in TP observed from the 1974-1991 period versus the 2001-2005 period (MDEQWB, 2010;
613 Supplementary Fig. 2). While DRP was not measured directly in the Saginaw River, the
614 modeling work done in this study indicates DRP concentrations for the Saginaw River are low in
615 comparison to those in the Maumee River, consistent with the lower TP levels (Figs. 5B, 6). The
616 higher proportion of wetlands and forest also help buffer the flow from the Saginaw River. The
617 combination of lower FWMC of P and less variable flow caused cyanobacterial blooms in
618 Saginaw Bay to be more consistent from year to year. Though reduced, there is still sufficient P
619 input to cause Saginaw Bay to be classified as eutrophic with blooms comparable to years with
620 low loading in the WLEB (Fig. 2B).

621 Another difference between the two systems is the extent of remaining wetland along their
622 shorelines. Saginaw Bay is bordered by 18,000 acres of wetlands (~73 km²), the largest coastal
623 freshwater wetlands system in the USA (USFWS, 2019). An important component of this
624 wetlands network is the wide swath of the three-square bulrush, *Schoenoplectus pungens*. This

625 species is known to act as a nutrient sink preventing large pulses of phosphorus from reaching
626 the open waters of the bay (Kohler et al., 2004). A review of 203 North American and European
627 wetlands reported median removal rates of $93 \text{ g m}^{-2} \text{ year}^{-1}$ for total nitrogen and $1.2 \text{ g m}^{-2} \text{ year}^{-1}$
628 of total phosphorus (Land et al., 2016). Assuming the median total phosphorus removal rates
629 reported by Land et al. (2016), Saginaw Bay's surrounding wetlands should remove 88 metric
630 tons (29%) of total phosphorus per year, compared to the average spring input of 300 metric tons
631 (IJC, 2019). This is sufficiently high to have a further ameliorating impact on reducing the
632 severity of cyanobacterial blooms in Saginaw Bay. Approximately 5,100 acres (20.6 km^2) of
633 Lake Erie's original wetlands remain in the WLEB. Using the same uptake assumptions, these
634 marshes could remove 25 metric tons P which is a small amount ($\sim 2\%$) compared to the average
635 1,126 metric tons discharged between March and June into the WLEB (Stumpf et al., 2016).

636 *4.2 Nonlinear response to phosphorus loading in western Lake Erie*

637 A critical feature of the response of TP loading in the WLEB that warrants consideration from a
638 management perspective is the non-linear response of cyanobacterial bloom intensity versus TP
639 input over 500 metric tons (Stumpf et al., 2012; Obenour et al. 2014; Bertani et al. 2016; Stumpf
640 et al., 2016; Verhamme et al., 2016; Ho et al. 2017). At TP loads less than 500 metric tons,
641 Saginaw Bay and the WLEB experience similar sized blooms (Fig. 2B, 5B, 6). In addition at
642 these lower TP loading levels there is a linear response of bloom size to the amount of TP input
643 (Fig. 5B). This raises the question of why TP loading exceeding 500 metric tons causes maximal
644 summertime cyanobacterial biomass to rise in a steep non-linear fashion (Fig. 5B). The
645 mechanism accounting for the non-linear response, however, has not been identified. A logical
646 hypothesis is that there is an internal cycling mechanism that causes the recent P inputs to be
647 utilized more effectively as loading increases (Gächter and Mares, 1985). A likely possibility is
648 that blooms of diatoms and other phytoplankton occurring in early summer are capable of
649 effectively sequestering incoming nutrients even in high flow years (Stoermer and Theriot, 1985;
650 Butts and Carrick, 2017; Reavie et al. 2018; O'Donnell et al., 2019). As water temperatures
651 increase in these shallow systems, the water column stabilizes, nutrients taken up by the initial
652 blooms can be remineralized directly via grazing or bacterial degradation as blooms senesce later

653 in the season (Kreusad et al., 2015; Bartoli et al. 2018; Depew et al. 2018; Null et al., 2020). In
654 essence, early blooms may provide a time release mechanism for initially capturing, then
655 supplying, highly utilizable DRP to support more intense cyanobacterial blooms later in the
656 season. This hypothesis is consistent with the cyanobacterial biomass pattern observed in WLEB
657 for the wetter years in 2011, 2013, 2015, 2017, and 2019 (Fig. 2B).

658 *4.3 Management implications for controlling cyanobacterial blooms in the WLEB*

659 From a management perspective, the Saginaw Bay watershed provides a realistic model for
660 further cyanobacterial abatement efforts in the WLEB. The results show that TP inputs into the
661 WLEB would have to drop below 500 metric tons to regularly produce cyanobacterial blooms
662 with comparable intensity to those observed in Saginaw Bay. This 500-metric ton threshold is
663 less than the current loading target of 860 metric tons for the WLEB (GLWQANAS, 2019).
664 Particular attention should be paid to reducing TP and DRP inputs as reflected in the Great Lakes
665 Water Quality Agreement Nutrients Annex (GLWQANAS, 2019). These reductions are
666 particularly important given the trend in increasing annual precipitation in the region over the
667 past several decades, which has the potential to escalate nutrient loading and bloom size (Stow et
668 al., 2015; Fig. 2). Consequently, target TP and DRP reductions may have to be even more drastic
669 than the 40% recommended in the GLWQANAS to achieve the desired reduction in bloom
670 intensity (Scavia et al. 2014; 2016; 2017; Iho et al., 2017; Smith et al. 2018; Wilson et al., 2018;
671 Baker et al., 2019). Numerous approaches for reducing P inputs have been proposed, but are
672 beyond the scope of this manuscript (e.g. Baker et al., 2017; King et al., 2018; Xia et al., 2020).
673 The non-linear response observed with loading in the WLEB means that initial reductions in the
674 highest P-loading rates will have the greatest benefit in terms of reducing bloom biomass (Fig.
675 5B). The largest loading observed in Saginaw Bay is just below the threshold where nonlinear
676 intensification of blooms would be expected to begin (Fig. 5B). Accordingly, increases in
677 agricultural land use or continued loss of wetlands in the Saginaw Bay watershed or surrounding
678 the Bay will significantly increase potential for severe cyanobacterial blooms (Mitsch and Wang,
679 2000; USFWS, 2019).

680 *4.4. Secondary influences on bloom intensity, retention time and water temperature*

681 Cyanobacteria blooms are caused by a combination of factors. The best documented of these are
682 temperature (Paerl and Huisman, 2009), residence (retention) times (Romo et al., 2013) and
683 eutrophication (Paerl, 1998). Michalak et al. (2013) showed that the large bloom present in the
684 WLEB in the summer of 2011 was partially a result of longer than usual residence times.
685 Summer mean residence time in the WLEB is reported to be 51 days (Millie et al., 2009). This is
686 a little less than half of the average summer residence time in Saginaw Bay, which is estimated
687 to be about 115 days for the entire bay and 62 days for the inner bay (Nguyen et al., 2014).
688 Therefore, residence times would indicate that Saginaw Bay should have larger blooms relative
689 to WLEB if all other factors were equal. This reinforces the importance of the relatively low TP
690 and estimated DRP concentrations in producing consistently moderate annual blooms in Saginaw
691 Bay where advective losses are lower. It also argues that any future increases in nutrient loading
692 will cause a more rapid and intense eutrophication of Saginaw Bay than occurs in the WLEB.

693 Temperatures in the two systems are similar to one another throughout the year and show little
694 interannual variability (Sayers et al., 2016; Supplementary Fig. 4). While there may be small
695 scale regional variability in the temperature data there was not sufficient temperature data to
696 work out differences from the time period encompassed in this study. Regression analysis failed
697 to show a correlation between temperature and maximum CI concentrations. Similarly, other
698 climatic drivers such as wind stress and light availability were not correlated with maximum CI
699 values. Temperature may, however, have affected the timing of the bloom which peaks 20 days
700 earlier in Saginaw Bay (Aug 11 - Aug 20) compared to the WLEB (Sep 1 - Sep 10) (Table 2).
701 Temperatures of 21.7 °C to 24 °C produce maximal potential *Microcystis* growth rates of 0.6 d⁻¹
702 to 0.69 d⁻¹. The average July temperatures for the WLEB and Saginaw Bay are 24.0 °C and 21.7
703 °C, respectively. In August the temperatures are 24.2 °C in the WLEB and 22.0 °C in Saginaw
704 Bay, and in September they decrease to 21.7 °C in the WLEB and 19.4 °C in Saginaw Bay.
705 Maximal *Microcystis* growth would correspondingly decrease to ~0.62 d⁻¹ in WLEB and ~0.5 d⁻¹
706 in Saginaw Bay. The continued warm temperatures in the WLEB support stronger growth into
707 September, which may explain why blooms peak later in WLEB compared to Saginaw Bay.
708 However, we cannot discount the possibility that another factor, such as nitrogen limitation could
709 be a factor in duration. Blooms in the WLEB generally switch from P-limitation to N-limitation

710 in August and September, possibly Saginaw Bay may experience nitrogen limitation earlier than
711 WLEB, which could promote bloom decline. However, this result could not be tested due to lack
712 of N data.

713 4.5. Temporal and geographic variation in bloom intensity in Saginaw Bay

714 On average the cyanobacterial bloom initiates during June and begins intensifying along the
715 southern and eastern shore in early July (Figs. 7, 8). The bloom fully develops mid-July though
716 the end of August, begins to dissipate in early September, and is gone by mid to late October.
717 The prevailing currents cause the bloom to be most intense along the shoreline with the middle
718 of the Bay relatively free of cyanobacteria. During the blooms, cyanobacterial concentrations are
719 highest along the southern shore adjacent to where the Saginaw River enters the bay (Fig. 9).
720 Concentrations along the eastern shore are also higher than those along the western shore,
721 consistent with the prevailing currents.

722 5. Conclusions

723 Saginaw Bay has less variable, lower biomass cyanobacterial blooms than the WLEB. This
724 difference is driven by lower and less variable P-inputs from the Saginaw River compared to the
725 Maumee River. Equivalent P-loading in both systems produced similar intensity blooms. A key
726 difference between the two systems is that the WLEB has TP loads exceeding 500 metric tons.
727 TP inputs into Saginaw Bay ranged from ~120-450 metric tons and overlapped levels observed
728 in the WLEB in lower input years. In this range, equivalent phosphorus loads produce equivalent
729 biomass blooms. Above 500 metric tons, cyanobacterial bloom biomass in the WLEB increases
730 rapidly in a non-linear fashion (Fig. 5B).

731 From a management perspective, these results indicate that reductions in TP loading, particularly
732 the DRP component, below the current maximal loading values in the WLEB will
733 disproportionately reduce boom intensity (Fig. 5B). If loading into the WLEB were reduced to
734 approximately 500 metric tons, blooms would be expected to be equivalent to those observed in
735 Saginaw Bay. Conversely, if P-inputs in Saginaw Bay are increased because of some factor, such
736 as a shift toward more intense agricultural land use, or additional destruction of wetlands, the

737 blooms are likely to intensify significantly. The highest P-inputs into Saginaw Bay are already
738 near the 500 metric tons P threshold and it is reasonable to predict loads above this threshold will
739 begin to produce non-linear intensification of cyanobacterial blooms.

740 Acknowledgements

741 This work was partially supported by the U.S. EPA Great Lakes Research Initiative. Andrew
742 Meredith maintains the image processing system. The authors would like to thank Bryan Eder
743 for assistance in making the map in Figure 1.

744

745

746 **References:**

- 747 Baker, D.B., Confesor, R., Ewing, D.E., Johnson, L.T., Kramer, J.W., Merryfield, N.J., 2014.
748 Phosphorus loading to Lake Erie from the Maumee, Sandusky, and Cuyahoga rivers: The
749 importance of bioavailability. *J. Great Lakes Res.* 40, 5502-517.
- 750 Baker, D.B., Johnson, L.T., Confessor, R.B., Crumrine, J.P., 2017. Vertical stratification of soil
751 phosphorus as a concern for dissolved phosphorus runoff in the Lake Erie Basin. *J.*
752 *Environ. Qual.* 46, 1287–1295.
- 753 Baker, D.B., Johnson, L.T., Confesor, Jr., R.B., Crumrine, J.P., Guo, T., Manning, N.F., 2019.
754 Early-term adjustments for Lake Erie phosphorus target loads to address western basin
755 cyanobacterial blooms. *J. Great Lakes Res.* 45, 203-211.
- 756 Bartoli, M., Zilius, M., Bresciani, M., Vaiciute, D., Vybernaite-Lubiene, I., Petkuvienė, J.,
757 Giordani, G., Daunys, D., Ruginis, T., Benelli, S., Giardino, C., Bukaveckas, P.A.,
758 Zemlys, P., Griniene, E., Gasiunaite, Z.R., Lesutiene, J., Pilkaitytė, R. Baziukas-
759 Razinkovas, A., 2018. Drivers of cyanobacterial blooms in a hypertrophic lagoon. *Front.*
760 *Mar. Sci.* <https://doi.org/10.3389/fmars.2018.00434>

- 761 Bierman, V.J., Dolan, D.M., Kasprzyk, R., Clark, J.L., 1984. Retrospective analysis of the
762 response of Saginaw Bay, Lake Huron to reductions in phosphorus loadings. Environ.
763 Sci. Technol. 18, 23-31.
- 764 Bertani, I., Obenour, D.R., Stegar, C.E., Stow, C.A., Gronewold, A.D., Scavia, D., 2016.
765 Probabilistically assessing the role of nutrient loading in harmful algal bloom formation
766 in western Lake Erie. J. Great Lakes Res. 42, 1184-1192.
- 767 Boedecker, A.R., Niewinski, D.N., Newell, S.E., Chaffin, J.D., McCarthy, M.J., 2020.
768 Evaluating sediments as an ecosystem service in western Lake Erie via quantification of
769 nutrient cycling pathways and selected gene abundances. J. Great Lakes Res. 46(4), 920-
770 932.
- 771 Bosse, K.R., Sayers, M.J., Shuchman, R.A., Fahnenstiel, G.A., Ruberg, S.A., Fanslow, D.L.,
772 Stuart, D.G., Johengen, T.H., Burtner, A.M. 2019. Spatio-temporal variability of in situ
773 cyanobacteria vertical structure in western Lake Erie: Implications for remote sensing
774 observations. J. Great Lakes Res. 45, 480-489.
- 775 Brooks, B.W., Lazorchak, J.M., Howard, M.D.A., Johnson, M.V., Morton, S.L., Perkins,
776 D.A.K., Reavie, E.D., Scott, G.I., Smith, S.A., Steevens, J.A., 2016. Are harmful algal
777 blooms becoming the greatest inland water quality threat to public health and aquatic
778 ecosystems? Environ. Toxicol. Chem. 35, 6-13.
- 779 Budd, J.W., Drummer, T.D., Nalepa, T.F., Fahnenstiel, G.L., 2001. Remote Sensing of biotic
780 effects: Zebra mussels (*Dreissena polymorpha*) influence on water clarity in Saginaw
781 Bay, Lake Huron. Limnol. Oceanogr. 46, 213-223.
- 782 Butts, E., Carrick, H.J., 2017. Phytoplankton Seasonality along a Trophic Gradient of Temperate
783 Lakes: Convergence in Taxonomic Composition during Winter Ice-Cover. Northeastern
784 Naturalist, 24(sp7):B167-B187. Eagle Hill Institute. <https://doi.org/10.1656/045.024.s719>

785 Cha, Y., Stow, C.A., Reckhow, K.H., DeMarchi, C., Johnengen, T.H., 2010. Phosphorus load
786 estimation in the Saginaw River, MI using a Bayesian hierarchical/multilevel model.
787 Water Res. 44, 3270-3282.

788 Chaffin, J.D., Bridgeman, T.B., Bade, D.L., 2013. Nitrogen constrains the growth of late summer
789 cyanobacterial blooms in Lake Erie. Adv. Microbiol. 3, 16–26.
790

791 Chaffin, J.D., Davis, T.W., Smith, D.J., Baer, M.M., Dick, G.J., 2018. Interactions between
792 nitrogen form, loading rate, and light intensity on Microcystis and Planktothrix growth
793 and microcystin production. Harmful Algae 73, 84–97.

794 Chorus, I., Bartram, J., 1999. Toxic Cyanobacteria in Water: A Guide to Their Public Health
795 Consequences, Monitoring and Management. World Health Organization, London, UK.

796 Clark, J.M., Schaeffer, B.A., Darling, J.A., Urquhart, E.A., Johnson, J.M., Ignatius, A.R., Myer,
797 M.H., Loftin, K.A., Werdell, J., Stumpf, R.P., 2017. Satellite monitoring of
798 cyanobacterial harmful algal bloom frequency in recreational waters and drinking water
799 sources. Ecol. Indic. 80, 84-95.

800 Conley, D.J., Paerl, H.W., Howarth, R.W., Boesch, D.F., Seitzinger, S.B., Havens, K.E.,
801 Lancelot, C., Likens, G.E., 2009. Controlling eutrophication: nitrogen and phosphorus.
802 Science 323, 1014-1015.

803 Davis T. W., Stumpf R., Bullerjahn G. S., McKay R. M. L., Chaffin J. D., Bridgeman T. B.,
804 Winslow, C., 2019. Science meets policy: a framework for determining impairment
805 designation criteria for large waterbodies affected by cyanobacterial harmful algal
806 blooms. Harmful Algae 81, 59–64. 10.1016/j.hal.2018.11.016

807 Davis, T.W., Watson, S.B., Rozmarynowycz, M.J., Ciborowski, J.J.H., McKay, R.M.,
808 Bullerjahn, G.S. 2014. Phylogenies of microcystin-producing cyanobacteria in the lower
809 Laurentian Great Lakes suggest extensive genetic connectivity. PLOS ONE.
810 <https://doi.org/10.1371/journal.pone.0106093>

811 Depew, D.C., Koehler, G., Hiriart-Baer, V., 2018. Phosphorus dynamics and availability in the
812 nearshore of eastern Lake Erie: Insights from oxygen isotope ratios of phosphate. *Front.*
813 *Mar. Sci.* <https://doi.org/10.3389/fmars.2018.00215>

814 Fishman, D.B., Adlerstein, S.A., Vanderploeg, H.A., Fahnenstiel, G.L., Scavia, D., 2010.
815 Phytoplankton community composition of Saginaw Bay, Lake Huron, during the zebra
816 mussel (*Dreissena polymorpha*) invasion: A multivariate analysis. *J. Great Lakes Res.*
817 36, 9-19.

818 Gächter, R., Mares, A., 1985. Does settling seston release-soluble reactive phosphorus in the
819 hypolimnion of lakes? *Limnol. Oceanogr.* 30, 364-371.

820 Gardner, W.S., Yang, L., Cotner, J.B., Johengen, T.H., Lavrentyev, P.J., 2001. Nitrogen
821 dynamics in sandy freshwater sediments (Saginaw Bay, Lake Huron). *J. Great Lakes Res.*
822 27, 84-97.

823 GES-DISC Interactive online visualization and analysis infrastructure (Giovanni), 2020.
824 Giovanni.gsfc.nasa.gov. Last accessed online 5/20/2020.

825 Gobbler, C.J., Burkholder, J.M., Davis, T.W., Harke, M.J., Johengen, T., Stow, C.A., Van de
826 Waal, D.B., 2016. The dual role of nitrogen supply in controlling the growth and toxicity
827 of cyanobacterial blooms. *Harmful Algae* 54, 87-97.

828 Gorham, T., Jia, Y., Shum, C.K., Lee, J. 2017. Ten-year survey of cyanobacterial blooms in
829 Ohio's waterbodies using satellite remote sensing. *Harmful Algae*. 66:13-19.

830 Gower, J., King, S., 2007. Validation of chlorophyll fluorescence derived from MERIS on the
831 west coast of Canada. *Int. J. Remote Sens.* 28(3), 625-635.

832 Great Lakes Water Quality Agreement Nutrients Annex Subcommittee (GLWQANAS), 2019.
833 Lake Erie Binational Phosphorus Reduction Strategy. [https://binational.net/wp-](https://binational.net/wp-content/uploads/2019/06/19-148_Lake_Erie_Strategy_E_accessible.pdf)
834 [content/uploads/2019/06/19-148_Lake_Erie_Strategy_E_accessible.pdf](https://binational.net/wp-content/uploads/2019/06/19-148_Lake_Erie_Strategy_E_accessible.pdf). Last accessed
835 4/25/2020.

836 Hallegraeff, G.M., 1993. A review of harmful algal blooms and their apparent global increase.
837 *Phycologia* 32, 79-99.

838 Hampel, J.J., McCarthy, M.J., Neudeck, M., Bullerjahn, G.S., McKay, R.M.L., Newell, S.E.,
839 2019. Ammonium recycling supports toxic *Planktothrix* blooms in Sandusky Bay, Lake
840 Erie: Evidence from stable isotope and metatranscriptome data. *Harmful Algae* 81, 42–
841 52.

842 Hawley, N. Redder, T., Beletsky, R., Verhamme, E., Beletsky, D., DePinto, J., 2014. Sediment
843 resuspension in Saginaw Bay. *J. Great Lakes Res.* 40, 18-27.

844 Heath, R.T., Fahnenstiel, G.L., Gardner, W.S., Cavaletto, J.F., Hwang, S., 1995. Ecosystem-level
845 effects of zebra mussels (*Dreissena polymorpha*) and enclosure experiment in Saginaw
846 Bay, Lake Huron. *J. Great Lakes Res.* 21, 501-516.

847 Heidelberg University National Center for Water Quality Research, 2019.
848 <https://ncwqr.org/monitoring/data/>. Last accessed 5/26/2020.

849 Hilborn, E.D., Beasley, V.R., 2015. One health and cyanobacteria in freshwater systems: Animal
850 illnesses and deaths are sentinel events for human health risks. *Toxins.* 7, 1374-1395.

851 Ho, J.C., Stumpf, R.P., Bridgeman, T.B., Michalak, A.M., 2017b. Using Landsat to extend the
852 historical record of lacustrine phytoplankton blooms: a Lake Erie case study. *Remote*
853 *Sens. Environ.* 191, 273–285.

854 Ho, J.C., Michalak, A.M., Pahlevan, N., 2019. Widespread global increase in intense lake
855 phytoplankton blooms since the 1980s. *Nature* 574, 667–670.

856 Horst, G.P., Sarnelle, O., White, J.D., Hamilton, S.K., Kaul, R.B. and Bressie, J.D., 2014.
857 Nitrogen availability increases the toxin quota of a harmful cyanobacterium, *Microcystis*
858 *aeruginosa*. *Water Research*, 54, pp.188-198.

859 Iho, A., Ahlvik, L., Ekhyolm, P., Lehtoranta, J., Kortelainen, P., 2017. Optimal phosphorus
860 abatement redefined: insights from coupled element cycles. *Ecol. Econ.* 137, 13–19.

861 International Joint Commission (IJC), 2019. The coastal wetlands of Lake Erie: Have we lost
862 our Swiss Army knife? Water Matters Newsletter. [https://www.ijc.org/en/coastal-](https://www.ijc.org/en/coastal-wetlands-western-lake-erie-have-we-lost-our-swiss-army-knife)
863 [wetlands-western-lake-erie-have-we-lost-our-swiss-army-knife](https://www.ijc.org/en/coastal-wetlands-western-lake-erie-have-we-lost-our-swiss-army-knife). Last accessed 5/20/2020.

864 Jarvie, H.P., Johnson, L.T., Sharpley, A.N., Smith, D.R., Baker, D.B., Bruulsema, T.W.,
865 Confesor, R., 2017. Increased soluble phosphorus loads to Lake Erie: Unintended
866 consequences of conservation practices? *J. Environ. Qual.* 46, 123–132.

867 Kane, D.D., Conroy, J.D., Richards, R.P., Baker, D.B., Culver, D.A., 2014. Re-eutrophication of
868 Lake Erie: correlations between tributary nutrient loads and phytoplankton biomass. *J.*
869 *Great Lakes Res.* 40, 496–501.

870 King, K.W., Williams, M.R., Macrae, M.L., Fausey, N.R., Frankenberger, J., Smith, D.R.,
871 Kleinman, P.J., Brown, L.C., 2015a. Phosphorus transport in agricultural subsurface
872 drainage: a review. *J. Environ. Qual.* 44, 467–485.

873 King, K.W., Williams, M.R., Fausey, N.R., 2015b. Contributions of systematic tile drainage to
874 watershed scale phosphorus transport. *J. Environ. Qual.* 44, 486–494.

875 King, K.W., Williams, M.R., LaBarge, G.A., Smith, D.R., Reutter, J.M., Duncan, E.W., Pease,
876 L.A., 2018. Addressing agricultural phosphorus loss in artificially drained landscapes
877 with 4R nutrient management practices. *J. Soil Water Conserv.* 73, 35–47.

878 Kohler, E.A., Poole, V.L., Reicher, Z.J., Turco, R.F., 2004. Nutrient, metal, and pesticide
879 removal during storm and nonstorm events by a constructed wetland on an urban golf
880 course. *Ecol. Eng.* 23, 285-298.

881 Kreuzad, M., Scharta, M., Enge, A., Nausc, M., Vos, M., 2015. Variations in the elemental ratio
882 of organic matter in the central Baltic Sea: Part I—Linking primary production to
883 remineralization. *Cont. Shelf Res.* 100, 25-45.

884 Land, M., Graneli, W., Grimvall, A., Hoffman, C.C., Mitsch, W.J., Tonderski, K.S., Verhoeven,
885 J.T.A., 2016. How effective are created or restored freshwater wetlands for nitrogen and

886 phosphorus removal? A systematic review. *Environ. Evid.* 5:9.
887 <https://doi.org/10.1186/2047-2382-2-16>

888 Lunetta, R.S., Schaeffer, B.A., Stumpf, R.P., Jacobs, S.A., Murphy, M.S., 2015. Evaluation of
889 cyanobacteria cell count detection derived from MERIS imagery across the eastern USA.
890 *Remote Sens. Environ.* 157, 24-34.

891 Manning, N. F., Wang, Y., Long, C. M., Bertani, I., Sayers, M., Bosse, K., Shuchman, R., and
892 Scavia, D. 2019. Extending the forecast model: Predicting Western Lake Erie harmful
893 algal blooms at multiple spatial scales. *Journal of Great Lakes Research*, 45(3), 587-595.

894 Michalak, A.M., Anderson, E.J., Beletsky, D., Boland, S., Bosch, N.S., Bridgeman, T.B.,
895 Chaffin, J.D., Cho, K., Confesor, R., Daloglu, I., DePinto, J.V., Evans, M.A., Fahnenstiel,
896 G.L., He, L., Ho, J.C., Jenkins, L., Johnengenjep, T.H., Kuo, K.C., LaPorte, E., Liu, X.,
897 McWilliams, M.R., Moore, M.R., Posselt, D.J., Richards, R.P., Scavia, D., Steiner, A.L.,
898 Verhamme, E., Wright, D.M., Zagorski, M.A., 2012. Record-setting algal bloom in Lake
899 Erie caused by agricultural meteorological trends consistent with expected future
900 conditions. *Proc. Natl. Acad. Sci. USA* 110, 6448-6452.

901 Michigan Department of Environmental Quality Water Bureau (MDEQWB), 2010. Update of
902 phosphorus load data for Saginaw Bay. MI/DEQ/WB-10/006. [https://www.baycounty-](https://www.baycounty-mi.gov/Docs/DrainComm/Approved%20WMP/Appendix_L.pdf)
903 [mi.gov/Docs/DrainComm/Approved%20WMP/Appendix_L.pdf](https://www.baycounty-mi.gov/Docs/DrainComm/Approved%20WMP/Appendix_L.pdf). Last accessed
904 5/27/2020.

905 Millie, D.F., Fahnenstiel, G.L., Dyble Bressie, J., Pigg, R.J., Rediske, R.R., Klarer, D.M., Tester,
906 P.A., Litaker, R.W., 2009. Late-summer phytoplankton in western Lake Erie (Laurentian
907 Great Lakes): bloom distributions, toxicity, and environmental influences. *Aquat. Ecol.*
908 43, 915-934.

909 Mishra, S., Stumpf, R.P., Schaeffer, B.A., Werdell, P.J., Loftin, K.A., and Meredith, A., 2019.
910 Measurement of cyanobacterial bloom magnitude using satellite remote sensing. *Sci Rep.*
911 9(1), 18310. doi:10.1038/s41598-019-54453-y

912 Mitsch, W.J., Wang, N., 2000. Large-scale coastal wetland restoration on the Laurentian Great
913 Lakes: Determining the potential for water quality improvement. *Ecol. Eng.* 15, 267-282.

914 Mitsch, W.J., 2017. Solving Lake Erie's harmful algal blooms by restoring the Great Black
915 Swamp in Ohio. *Ecological Engineering*. 108, 406-413.

916 National Aeronautics and Space Administration (NASA) SeaDAS Software Package, 2019.
917 <https://seadas.gsfc.nasa.gov/>. Last accessed 5/26/2020.

918 Newell, S.E., Davis, T.W., Johengen, T.H., Gossiaux, Burtner, A., Palladino, D., McCarthy,
919 M.J., 2019. *Harmful Algae*. 81, 86-93.

920 Nguyen, T.D., Thupaki, P., Anderson, E.J., Phanikumar, M.S., 2014. Summer circulation in the
921 Saginaw Bay –Lake Huron system. *J. Geophys. Res. Oceans*. 119, 2713-2734.

922 Null, G., Errera, R., Fanslow, D.L., 2020. OB14F-0426 - Identifying seasonal shifts in freshwater
923 phytoplankton assemblages through optimizing a flow imaging microscopy technology
924 for the Great Lakes. Ocean Sciences Meeting, 16-21 February, San Diego, CA USA.

925 Obenour, D.R., Gronewold, A.D., Stow, C.A., Scavia, D., 2014. Using a Bayesian hierarchical
926 model to improve Lake Erie cyanobacteria bloom forecasts. *Water Resour. Res.* 50,
927 7847-7860.

928 O'Donnell, D.R., Conine, A., Hood, J.M., 2019. Time Series Analysis of Lake Erie
929 Phytoplankton dynamics final report for the Ohio Lake Erie Commission, grant number
930 SG-531-2018.
931 [https://lakeerie.ohio.gov/Portals/0/LEPF/LEPF%20Final%20Report%20531-
932 18%20sm.pdf?ver=2020-02-10-151947-517](https://lakeerie.ohio.gov/Portals/0/LEPF/LEPF%20Final%20Report%20531-18%20sm.pdf?ver=2020-02-10-151947-517). Last accessed 5/26/2020.

933 Ohio Environmental Protection Agency (Ohio EPA), 2008. Evaluation of land use/land Cover
934 characteristics in Ohio drainages to Lake Erie. Ohio Phosphorus Task Force.
935 [https://www.epa.ohio.gov/portals/35/lakeerie/ptaskforce/OPTF_Landuse_20081001_hres
936 .pdf](https://www.epa.ohio.gov/portals/35/lakeerie/ptaskforce/OPTF_Landuse_20081001_hres.pdf). Last accessed 5/26/2020.

- 937 Paerl, H.W., 1988. Nuisance phytoplankton blooms in coastal, estuarine, and inland waters.
938 Limnol. Oceanogr. 33, 823-847.
- 939 Paerl, H.W., Huisman, J., 2008. Blooms like it hot. Science 320, 57-58.
- 940 Paerl, H.W., Huisman, J., 2009. Climate change: A catalyst for global expansion of harmful
941 cyanobacterial blooms. Environ. Microbiol. Rep. 1, 27-37.
- 942 Paerl, H.W., Paul, V.J., 2012. Climate change: Links to global expansion of harmful
943 cyanobacteria. Water Res. 46, 1349-1363.
- 944 Paerl, H.W., Otten, T.G., 2013. Harmful cyanobacterial blooms: causes, consequences, and
945 controls. Microb. Ecol. 65, 995-1010.
- 946 Paerl, H.W., Scott J.T., McCarthy M.J., Newell S.E., Gardner W.S., Havens K.E., Hoffman
947 D.K., Wilhelm S.W., Wurtsbaugh W.A. 2016. It takes two to tango: when and where dual
948 nutrient (N & P) reductions are needed to protect lakes and downstream ecosystems.
949 Environ. Sci. Technol. 50, 10805–10813.
- 950 Pillsbury, R.W., Lowe, R.L., Pan, Y.D., Greenwood, J.L., 2002. Changes in the benthic algal
951 community and nutrient limitation in Saginaw Bay, Lake Huron, during the invasion of
952 the zebra mussel (*Dreissena polymorpha*). J. N. Am. Benthol. Soc. 21, 238-252.
- 953 Pope, R.M., Fry, E.S., 1997. Absorption spectrum (380-700 nm) of pure water. II. Integrating
954 cavity measurements. Appl. Opt. 33, 8710-8723.
- 955 Reavie, E.D., Cai, M., Twiss, M.R., Carrick, H.J., Davis, T.W., Johengen, T.H., Gossiaux, D.,
956 Smith, D.E., Palladino, D., Burtner, A., Sgro, G.V., 2016. Winter-spring diatom
957 production in Lake Erie is an important driver of summer hypoxia. J. Great Lakes Res.
958 42, 608–618.
- 959 Reynolds, C.S., Oliver, R.L., Walsby, A.E., 1987. Cyanobacterial dominance: the role of
960 buoyancy regulation in dynamic lake environments. New Zeal. J. Mar. Fresh. Res. 21,
961 379-390.

962 Rockwell, D.C., G.J. Warren, P.E. Bertram, D.K. Salisbury, and N.M. Burns. 2005. The US EPA
963 indicators monitoring program 1983-2002: Trends in phosphorus, silica, and chlorophyll
964 a in the central basin. *J. Great Lakes Res.* 31, 23-34.

965 Romo, S., Soria, J., Fernandez, F., Ouahid, Y., Baron-Sola, A., 2013. Water residence time and
966 the dynamics of toxic cyanobacteria. *Freshw. Biol.* 58, 513-522.

967 Saginaw 2020; Source of Your Drinking Water [https://www.saginaw-](https://www.saginaw-mi.com/departments/wastewaterandwatertreatmentservices/watertreatment/sourceofyourdrinkingwater.php)
968 [mi.com/departments/wastewaterandwatertreatmentservices/watertreatment/sourceofyourdrinkingwater.php](https://www.saginaw-mi.com/departments/wastewaterandwatertreatmentservices/watertreatment/sourceofyourdrinkingwater.php). Last accessed September 20, 2020.

970 Sayers, M., Fahnenstiel, G.L., Shuchman, R.A., Whitley, M., 2016. Cyanobacteria blooms in
971 three eutrophic basins of the Great Lakes: a comparative analysis using remote sensing.
972 *Int. J. Remote Sens.* 37, 4148-4171.

973 Scavia, D., Allan, J.D., Arend, K.K., Bartell, S., Beletsky, D., Bosch, N.S., Brandt, S.B.,
974 Briland, R.D., Daloglu, I., DePinto, J.V., Dolan, D.M., Evans, M.A., Farmer, T.M., Goto,
975 D., Han, H., Hook, T.O., Knight, R., Ludsin, S.A., Mason, D., Michalak, A.M., Richards,
976 R.P., Roberts, J.J., Rucinski, D.K., Rutherford, E., Schwab, D.J., Sesterhenn, T.M.,
977 Zhang, H., Zhou, Y., 2014. Assessing and addressing the re-eutrophication of Lake Erie:
978 central basin hypoxia. *J. Great Lakes Res.* 40, 226–246.

979 Scavia, D., DePinto, J.V., Bertani, I., 2016, A multi-model approach to evaluating target
980 phosphorus loads for Lake Erie. *J. Great Lakes Res.* 42, 1130–1150.

981 Scavia, D., Kalcic, M., Muenich, R.L., Read, J., Aloysius, N., Bertani, I., Boles, C., Confessor,
982 R., DePinto, J., Gildow, M., Martin, J., Reddar, T., Robertson, D., Sowa, S., Wang, Y.,
983 Yen, H., 2017. Multiple models guide strategies for agricultural nutrient reductions.
984 *Front. Ecol. Environ.* 15, 126–132.

985 Schaeffer, B.A., Bailey, S.W., Comney, R.N., Galvin, M., Ignatius, A.R., Johnston, J.M., Keith,
986 D.J., Lunetta, R.S., Parmar, R., Stumpf, R.P., Urquhart, E.A., Werdell, P.J., Wolfe, K.,
987 2018. Mobile device application for monitoring cyanobacteria harmful algal blooms

988 using Sentinel-3 satellite Ocean and Land Colour Instruments. *Environ. Modell. Softw.*
989 109, 93-103.

990 Schaeffer, B. A., Loftin, K., Stumpf, R.P., Werdell, P. J., 2015. Agencies collaborate, develop a
991 cyanobacteria assessment network, *EOS* 96, doi:10.1029/2015EO038809.

992 Sigleo, A., Frick, W., 2003. Seasonal Variations in River Flow and Nutrient Concentrations in a
993 Northwestern USA Watershed. pp. 370-376. In: K.G. Renard, S.A. McElroy, W.J.
994 Gburek, H.E. Canfield, and R.L. Scott [eds.], First interagency conference on research in
995 the watersheds. U.S. Department of Agriculture.

996 Smayda, T.J. 1990. Novel and nuisance phytoplankton blooms in the sea: Evidence for a global
997 epidemic. pp 29-40. In: Graneli E. [ed.] *Toxic marine phytoplankton*, Elsevier, New
998 York, NY, USA.

999 Smith, D.R., King, K.W., Johnson, L., Francesconi, W., Richards, P., Baker, D., Sharpley, A.N.,
1000 2015a. Surface Runoff and Tile Drainage Transport of Phosphorus in the Midwestern
1001 United States. *Journal of Environmental Quality* 44(2), 495.

1002 Smith, D.R., King, K.W., Williams, M.R., 2015b. What is causing harmful algal blooms in Lake
1003 Erie? *J. Soil Water Conserv.* 70, 27A–29A.

1004 Smith, D.R., Wilson, R.S., King, K.W., Zwonitzer, M., McGrath, J.M., Harmel, R.D., Haney,
1005 R.L., Johnson, L.T., 2018. Lake Erie, phosphorus, and microcystin: is it really the
1006 farmer's fault? *J. Soil Water Conserv.* 73, 48–57.

1007 Smith, V.H., 1983. Low nitrogen to phosphorus ratios favor dominance by blue-green
1008 algae in lake phytoplankton. *Science* 221(4611), 669–671.

1009 Steffen, M.M., Belisle, B.S., Watson, S.B., Boyer, G.L., Wilhelm, S.W. 2014. Status, causes and
1010 controls of cyanobacterial blooms in Lake Erie. *J. Great Lakes Res.* 40, 215-225.

1011 Steffen, M.M., Davis, T.W., McKay, R.M., Bullerjahn, G.S., Krausfeldt, L.E., Stough, J.M.A.,
1012 Neitzey, M.L., Gilbert, N.E., Boyer, G.L., Johengen, T.H., Gossiaux, D.C., Burtner,
1013 A.M., Palladino, D., Rowe, M., Dick, G.J. Meyer, K., Levy, S., Boone, B., Stumpf, R.,
1014 Wynne, T.T., Zimba, P.V., Gutierrez, D.B., Wilhelm, S.W., 2017. Ecophysiological
1015 examination of the Lake Erie *Microcystis* bloom in 2014: linkages between biology and
1016 the water supply shutdown of Toledo, Ohio. *Environ. Sci. Technol.* 51, 6745-6755.

1017 Stoermer, E.F., Theriot, E., 1985. Phytoplankton Distribution in Saginaw Bay. *J. Great Lakes*
1018 *Res.* 11(2), 132-142.

1019 Stow, C.A., Dyble, J., Kashian, D.R., Johengen, T.H., Peters Winslow, K., Peacor, S.D.,
1020 Francour, S.N., Burtner, A.M., Palladino, D., Morehead, N., Gossiaux, D., Cha, Y.K.,
1021 Qian, S.S., Miller, D., 2014. Phosphorus targets and eutrophication objectives in Saginaw
1022 Bay: A 35 year assessment. *J. Great Lakes Res.* 40, 4-10.

1023 Stow, C. A., Y. Cha, L. T. Johnson, R. Confesor, and R. P. Richards. 2015. Long-term and
1024 seasonal trend decomposition of Maumee River nutrient inputs to western Lake Erie.
1025 *Environ. Sci. Technol.* 49: 3392–3400. doi:10.1021/es5062648

1026 Stumpf, R.P., Werdell, P.J., 2010. Adjustment of ocean color sensor calibration through multi-
1027 band statistics. *Opt. Express* 18, 401-412.

1028 Stumpf, R.P., Wynne, T.T., Baker, D.B., Fahnenstiel, G.L., 2012. Interannual variability of
1029 cyanobacterial blooms in Lake Erie. *PLOS ONE.* 7 e42444.

1030 Stumpf, R.P., Johnson, L.T., Wynne, T.T., Baker, D.B., 2016. Forecasting annual cyanobacterial
1031 bloom biomass to inform management decisions in Lake Erie. *J. Great Lakes Res.* 42,
1032 1174-1183.

1033 U.S. Fish and Wildlife Service (USFWS), 2019. Michigan Wetland Resources.
1034 <https://www.fws.gov/wetlands/data/Water-Summary-Reports/National-Water-Summary->
1035 [Wetland-Resources-Michigan.pdf](https://www.fws.gov/wetlands/data/Water-Summary-Reports/National-Water-Summary-Wetland-Resources-Michigan.pdf). Last accessed 5/26/2020.

- 1036 Urquhart, E.A., Schaeffer, B.A., Stumpf, R.P., Loftin, K.A., Werdell, P.J., 2017. A method for
1037 examining temporal changes in cyanobacteria harmful algal bloom spatial extent using
1038 satellite remote sensing. *Harmful Algae*. 67, 144-152.
- 1039 Vanderploeg, H.A., Jiebig, J.R., Carmichael, W. W., Agy, M.A., Johengen, T.H., Fahnenstiel,
1040 G.L., Nalepa, T.F., 2001. Zebra Mussel (*Dreissena polymorpha*) selective filtration
1041 promoted toxic *Microcystis* blooms in Saginaw Bay (Lake Huron) and Lake Erie. *Can. J.*
1042 *Fish. Aquat. Sci.* 58, 1208-1221.
- 1043 Verhamme, E.M., Redder, T.M., Schlea, D.A., Grush, J., Bretton, J.F., DePinto, J.V., 2016.
1044 Development of the Western Lake Erie Ecosystem Model (WLEEM): application to
1045 connect phosphorus loads to cyanobacteria biomass. *J. Great Lakes Res.* 42, 1193–1205.
- 1046 Wang, G., Lee, Z., and Mouw, C. 2018. Multi-spectral remote sensing of phytoplankton pigment
1047 absorption properties in cyanobacteria bloom waters: a regional example in the western
1048 basin of Lake Erie. *Remote Sensing*. 10(2), 302.
- 1049 Watson, S.B., Ridal, J., Boyer, G.L., 2008. Taste and odor can cyanobacterial toxins:
1050 Impairment, prediction, and management in the Great Lakes. *Can. J. Fish. Aquat. Sci.* 65,
1051 1779-1796.
- 1052 Williams, M.R. King, K.W., Ford, W., Buda, A.R., Kennedy, C.D. 2016. Effect of tillage on
1053 macropore flow and phosphorus transport to tile drains. *J. Environ. Qual.* 46, 1306–1313.
- 1054 Wilson, A.E., Wilson, W.A., Hay, M.E., 2006. Intraspecific variation in growth and morphology
1055 on the bloom-forming cyanobacterium *Microcystis aeruginosa*. *Appl. Environ.*
1056 *Microbiol.* 72, 7386-7389.
- 1057 Wilson, R.S., Beetstra, M.A., Reutter, J.M., Hesse, G., DeVanna-Fussell, K.M., Johnson, L.T.,
1058 King, K.W., LaBarge, G.A., Martin, J.F., Winslow, C., 2018. Commentary: achieving
1059 phosphorus reduction targets for Lake Erie. *J. Great Lakes Res.* 45(1):4-11.

- 1060 Withers, P.J.A., Jarvie, H.P., 2008. Delivery and cycling of phosphorus in rivers: A review. *Sci.*
1061 *Total Environ.* 400, 379-395.
- 1062 Wynne, T.T., Stumpf, R.P. 2015. Spatial and temporal patterns in the seasonal distribution of
1063 toxic cyanobacteria in western Lake Erie from 2002-2014. *Toxins* 7, 1649-1663.
- 1064 Wynne, T.T., Stumpf, R.P., Tomlinson, M.C., Warner, R.A., Tester, P.A., Dyble, J., Fahnenstiel,
1065 G.L. 2008. Relating spectral shape to cyanobacterial blooms in the Laurentian Great
1066 Lakes. *Int. J. Remote Sens.* 29, 3665–3672.
- 1067 Wynne, T.T., Stumpf, R.P., Tomlinson, M.C., Dyble, J., 2010. Characterizing a cyanobacterial
1068 bloom in western Lake Erie using satellite imagery and metrological data. *Limnol.*
1069 *Oceanogr.* 55, 2025–2036.
- 1070 Wynne, T.T., Stumpf, R.P., Tomlinson, M.C., Fahnenstiel, G.L., Schwab, D.J., Dyble, J.,
1071 Joshi, S., 2013a. Evolution of a cyanobacterial bloom forecast system in western Lake
1072 Erie: Development and initial evaluation. *J. Great Lakes Res.* 39, 90–99.
- 1073 Wynne, T.T., Stumpf, R.P. Briggs, T.O., 2013b. Comparing MODIS and MERIS spectral shapes
1074 for cyanobacterial bloom detection. *Int. J. Remote Sens.* 34, 6668–6678.
- 1075 Wynne, T.T., Meredith, A., Stumpf, R.P., Briggs, T.O., Litaker, R.W., 2018. Harmful algal
1076 bloom forecasting branch ocean color satellite imagery processing guidelines. NOAA
1077 Technical Memorandum NOS NCCOS 252.
1078 <https://repository.library.noaa.gov/view/noaa/20270>. Last accessed 5/20/2020.
- 1079 Xu, H., Paerl, H.W., Qin, B., Zhu, G., Gaia, G., 2009. Nitrogen and phosphorus inputs control
1080 phytoplankton growth in eutrophic Lake Taihu, China. *Limnol. Oceanogr.* 55, 420-432.
- 1081 You, J., Mallery, K., Hong, J., Hondzo, M. 2018, Temperature effects on growth and buoyancy
1082 of *Microcystis aeruginosa*. *J. Plank. Res.* 40(1), 16–28.

1083 Young, T.C., DePinto, J.V., Martin, S.C., Bonner, J.S., 1985. Algal-available particulate
1084 phosphorus in the Great Lakes Basin. *J. Great Lakes Res.* 11, 434–446.

1085 Zhang, F., Hu, C., Shum, C.K., Liang, S. and Lee, J. 2017. Satellite remote sensing of drinking
1086 water intakes in Lake Erie for cyanobacteria population using two MODIS-based
1087 indicators as a potential tool for toxin tracking. *Front. Mar. Sci.*
1088 <https://doi.org/10.3389/fmars.2017.00124>

1089

1090 **Figure Legends**

1091 Figure 1. Maps of the two study areas. (Top) Bathymetry and other relevant features of Saginaw
1092 Bay. (Middle) Geographic location of Saginaw Bay and the WLEB relative to one another. The
1093 Saginaw and Maumee Rivers supply a majority of the nutrients to Saginaw Bay and the WLEB
1094 respectively. (Bottom) The bathymetry and other relevant features of the WLEB.

1095 Figure 2. Monthly variations in cyanobacterial biomass in Saginaw Bay and the WLEB. (A) The
1096 maximal cumulative cyanobacterial index (CI) values from every 10-day composite (see Table 1)
1097 available for Saginaw Bay for 2000-2019. (B) The maximal commutative CI values for the
1098 WLEB (light bars) and Saginaw Bay (dark bars) allowing comparison of relative differences in
1099 the biomass of the cyanobacterial blooms in the two systems. The vertical black lines delimit the
1100 bloom season for each year, which starts on June 1 – June 10 and ends October 20-October 31
1101 (See Table 1). Each bloom year was divided into the same 15, 10-day composite periods.

1102 Figure 3. Relationship between the maximal annual CI value (*) in Saginaw Bay and cumulative
1103 volumetric output from the Saginaw River for the time periods. Circles (-o-) indicate volumetric
1104 output per water year which is October previous year to September of the current year. This
1105 encompasses the progression of annual blooms from their demise in October in one year through
1106 the summertime bloom and late summer/early fall decline the following year. Symbols (...+...)
1107 represents volumetric output of the Saginaw River from March - June and (-x-) the March - July
1108 output.

1109 Figure 4. Monthly discharge from the Saginaw and Maumee Rivers. (A) Mean and standard
1110 deviation for monthly discharge from the Saginaw River between 2000-2019. The data are
1111 plotted from October 1 to September 30 to correspond to the end of the bloom the previous year
1112 and the decline of the bloom the following September. (B) Same data for the Maumee River
1113 processed as detailed in A.

1114 Figure 5. Relationship between (A) March - June discharge from the Saginaw and Maumee
1115 Rivers from 2000-2008 and (B) March - June total phosphate loading (from 2000-2008) from the
1116 Saginaw and Maumee Rivers versus the corresponding maximal 10-day Cyanobacterial Index in
1117 Saginaw Bay (*) and the WLEB (o), respectively.

1118 Figure 6. Observed annual maximum 10-day, Cyanobacterial Index (CI) values vs modeled
1119 maximal CI based on total phosphorus (TP) input from the Maumee (o) and Saginaw (*) Rivers.
1120 The models used for predicting CI from TP were originally developed using data available for
1121 the WLEB (Stumpf et al. 2016). The diagonal line indicates a 1:1 correspondence between actual
1122 and modeled maximum CI values.

1123 Figure 7. Time series showing the average maximal Cyanobacterial Index (CI) values for every
1124 pixel in Saginaw Bay obtained for each of the 15, ten-day periods in a bloom season (Table 1).
1125 Warmer colors indicate higher levels of cyanobacteria, while cooler colors indicate lower levels.
1126 The composited images for each 10-day period were then arranged in chronological order to
1127 show development and decline of the bloom. Data for each image were determined by extracting
1128 the maximal CI values for the same pixel in every corresponding 10-day period between 2000
1129 and 2019 and then averaging those data to provide a mean pixel value for a given 10-day period
1130 across all years. The center of the bay has lower cyanobacterial concentrations relative to the
1131 shoreward areas due to prevailing circulation within the bay. The inner bay also has higher
1132 concentration relative to the outer bay.

1133 Figure 8. Time series showing the percent of the years in the study maximal Cyanobacterial
1134 Index (CI) values for every pixel in Saginaw Bay exceeded one of two thresholds. (A) The
1135 percent of time a pixel exceeded a (CI) of 0 in each of the 15, ten-day periods in a bloom season

1136 over the 20 year cyanobacterial time series from Saginaw Bay. A CI=0 is estimated to be
1137 ~20,000 cells mL⁻¹ (Stumpf et al., 2012). This graphic provides a probability estimate of a
1138 cyanobacterial bloom being present in a given location in each of the 15 of the 10-day periods
1139 from June 1 to October 31. (B) Same as A except it is percent of time the CI value was ≥ 0.001,
1140 which is equivalent to a concentration of 10⁵ cells mL⁻¹.

1141 Figure 9. (A) Saginaw Bay was subdivided into 5 regions to examine geographic variation in
1142 bloom intensity. The cumulative maximal CI values for each 10-day composites from each of
1143 these five regions was then plotted as time series from 2000 to 2019. (B) Map showing the
1144 different subregions of the Bay. (C) The average of the cumulative maximal CI values for each
1145 subregion over all 20 years of the study normalized to surface area. Region 1, closest to the
1146 primary nutrient source, the Saginaw River, had the highest CI value. The inner bay (R2, R3),
1147 had a higher CI value than the outer bay subregions (R4, R5). Values for the eastern shore
1148 subregions (R3, R5) were higher than the corresponding ones on the eastern shore (R2, R4).

1149

1150 Supplementary Fig. 1. March to July loads of total phosphorus load versus total bioavailable
1151 phosphorus for the Maumee River.

1152 Supplementary Fig. 2. (A) Regression analysis of the relationship between annual volume of
1153 water from the Saginaw River and total annual phosphorus load from the 1974- 1991
1154 (MDEQWB, 2010) (B) Same as for (A) except for the 2001-2005 time period (MDEQWB,
1155 2010). The slope of the regression lines represents the flow weighted mean concentration
1156 (FWMC) of TP (mg mL⁻¹) for both time periods. The differences in the FWMC concentrations
1157 during the two periods are consistent with phosphorus abatement strategies begun in the 1970s
1158 having reduced TP loading into Saginaw Bay from the Saginaw River by 37% in the early to
1159 mid-2000s.

1160 Supplementary Fig. 3. Regression analysis of the CI from the Stumpf et al. (2016) model on
1161 western Lake Erie against the CI from the MODIS data used in the current study. The slope (m)
1162 and the slope intercept (b) of the relationship shown here was used to adjust equation 6.

1163 Supplementary Fig. 4. Relationship between mean monthly water temperature in the WLEB
1164 versus Saginaw Bay from 2002-2019.

1165

1166 Tables

1167 *Table 1: The 10-day composite numbering system used for each year in both Saginaw Bay and*
1168 *western Lake Erie basin.*

Composite Number	Start Date	End Date
1	June 1	June 10
2	June 11	June 20
3	June 21	June 30
4	July 1	July 10
5	July 11	July 20
6	July 21	July 31
7	August 1	August 10
8	August 11	August 20
9	August 21	August 31
10	September 1	September 10

11	September 11	September 20
12	September 21	September 30
13	October 1	October 10
14	October 11	October 20
15	October 21	October 31

1169

1170 *Table 2: The 10-day composite periods (in parentheses) exhibiting the highest mean, median,*
 1171 *and mode integrated CI values during the 20-year MODIS time series. Details on how values*
 1172 *were calculated are given in section 2.3.*

Statistic	western Lake Erie Basin	Saginaw Bay
Mean ± SD	9.7 ± 2.4 (Sep 1 - Sep 10)	7.75± 1.7 (Aug 11 - Aug 20)
Median	10.0 (Sep 1 - Sep 10)	7.5 (Aug 11 - Aug 20)
Mode	10.0 (Sep 1 - Sep 10)	9.0 (Aug 21 - Aug 31)

1173

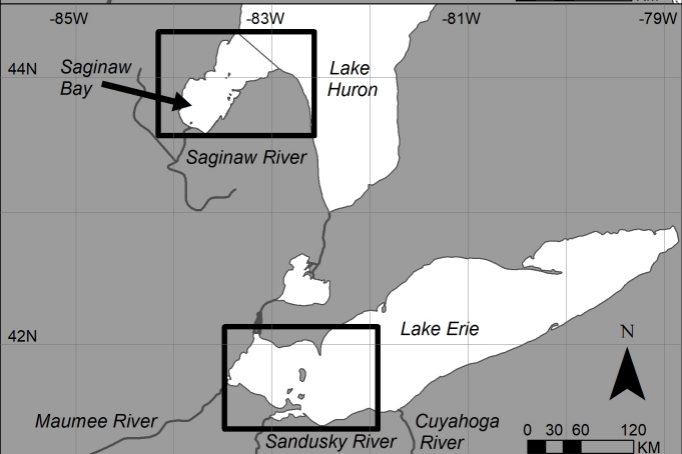
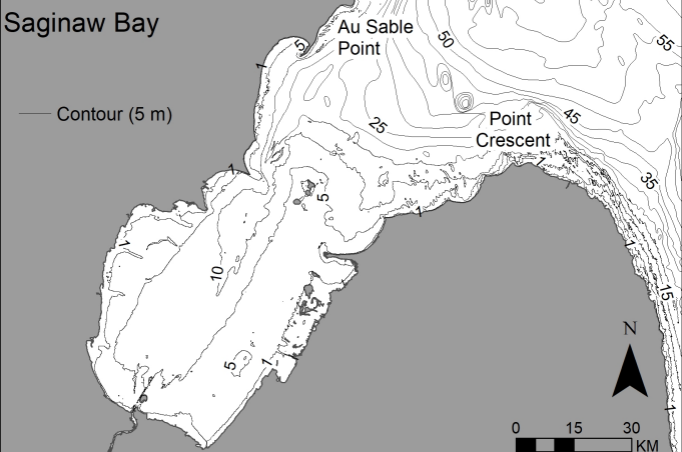
1174

1175

1176

1177

Saginaw Bay



Western Lake Erie

